

**AN EXPERIMENTAL STUDY ON
IMPROVEMENT OF A SAVONIUS ROTOR
PERFORMANCE WITH MULTIPLE HALVES
BLADES**

**A THESIS SUBMITTED TO THE GRADUATE
SCHOOL OF APPLIED SCIENCES**

OF

NEAR EAST UNIVERSITY

By

Mohanad H. M. Al Ghriyah

**In Partial Fulfillment of the Requirements for
the Degree of Master of Science
in
Mechanical Engineering**

NICOSIA, 2017

Mohanad Al Ghriyah

AN EXPERIMENTAL STUDY ON IMPROVEMENT OF A SAVONIUS ROTOR PERFORMANCE
WITH MULTIPLE HALVES BLADES

NEU
2017

**AN EXPERIMENTAL STUDY ON IMPROVEMENT
OF A SAVONIUS ROTOR PERFORMANCE WITH
MULTIPLE HALVES BLADES**

**A THESIS SUBMITTED TO THE GRADUATE
SCHOOL OF APPLIED SCIENCES**

OF

NEAR EAST UNIVERSITY

By

Mohanad Al Ghriyah

**In Partial Fulfillment of the Requirements for
the Degree of Master of Science
in
Mechanical Engineering**

NICOSIA, 2017

**Mohanad Al GHRIYBAH: AN EXPERIMENTAL STUDY ON IMPROVEMENT
OF A SAVONIUS ROTOR PERFORMANCE WITH MULTIPLE HALVES
BLADES**

**Approval of Director of Graduate School of
Applied Sciences**

Prof. Dr. Nadire ÇAVUŞ

**We certify this thesis is satisfactory for the award of the degree of master of science in
Mechanical Engineering**

Examining Committee in Charge:

I hereby declare that, all the information in this document has been obtained and presented in accordance with academic rules and ethical conduct. I also declare that, as required by these rules and conduct, I have fully cited and referenced all material and results that are not original to this work.

Name, Last Name :

Signature :

Date:

ACKNOWLEDGEMENT

I would like to especially thank my thesis advisor, Assist. Prof. Dr. Hüseyin ÇAMUR, for his useful guidance and supporting me with valuable information and discussions that assisted me in working through many problems.

I would like to thank M.Sc Youssef Kassem for guiding me through the experimental method and his valuable advice on several issues.

Lastly I must thank my parents and brothers who have encouraged me to hold on, especially when my morale was low from. I also thank all of my friends both here in and in Jordan for providing everything I need.

Thank you for all unconditional support with my studies

ABSTRACT

Savonius rotor is preferred for many power generation applications like tidal, wind and hydro, especially on a small scale by virtue of its simple and inexpensive construction, installation and maintenance. This study focuses on the measurement and comparison of the performance in terms of static torque and mechanical power of two new configuration of the Savonius rotor with the conventional one. Both configuration comprises a multiple halves blade with various positions and blade geometries added to the conventional configuration. In this research, the rotors with different configurations were located in front of the open wind tunnel and the tests were repeated four times in order to reduce errors. The experimental results showed that halves blade geometries affect the performance of new designs of Savonius rotors. Moreover, both configuration were produced more mechanical power than the conventional Savonius rotor. The results indicated that the static torque and mechanical power of the first configuration of Savonius rotors is higher than other configuration.

Keyword: Savonius rotors; new configuration; Static torque; mechanical power; Halves blades

ÖZET

Savonius rotor gel-git, rüzgar ve hidro gibi pek çok enerji üretimi uygulamaları için, özellikle basit ve ucuz yapım, kurulum ve bakım sayesinde küçük bir ölçekte tercih edilmektedir. Bu çalışma Savonius rotorunun iki yapılandırmasının statik tork ve mekanik güç açısından geleneksel bir rotor ile ölçülmesi ve karşılaştırılması üzerine odaklanmaktadır. Her iki yapılandırma da çeşitli konumlara sahip çoklu yarım bir bıçak (pervane) ve geleneksel yapılandırmaya eklenmiş bıçak geometrilerinden oluşmaktadır. Bu araştırmada, farklı yapılandırmalara sahip rotorlar açık rüzgar tünelinin önüne yerleştirilmiş ve hataları azaltmak için testler dört kez tekrar edilmiştir. Deney sonuçları, yarım bıçak geometrilerinin Savonius rotorlarının yeni tasarımlarının performansını etkilediğini göstermiştir. Ayrıca, her iki yapılandırmada da geleneksel Savonius rotorundan daha fazla mekanik güç üretilmiştir. Sonuçlar, Savonius rotorlarının ilk yapılandırmasının statik torkunun ve mekanik gücünün diğer yapılandırmadan daha yüksek olduğunu göstermiştir.

Anahtar Kelimeler: Savonius rotorları; Yeni yapılandırma; Statik tork; Mekanik güç; Yarım bıçaklar (pervaneler)

TABLE OF CONTENTS

ACKNOWLEDGEMENT	ii
ABSTRACT	iv
ÖZET	v
TABLE OF CONTENTS	vi
LIST OF TABLES	ix
LIST OF FIGURES	x
LIST OF SYMBOLS	xiii
CHAPTER 1: INTRODUCTION	1
1.1 Background of the Study	1
1.2 Research Goals	1
1.3 Research Outline	2
CHAPTER 2: WIND TURBINE FUNDAMENTAL	3
2.1 History of Wind Turbines	3
2.2 Turbine Classification	3
2.2.1 Horizontal Axis Wind Turbines	3
2.2.2 Vertical Axis Wind Turbines	5
2.2.2.1 Savonius Rotor	6
2.2.2.2 Darrieus Wind Turbine	7
2.3 VAWT Advantages and Applications	8
2.5 Drag type and lift type wind turbines	9
CHAPTER 3: EXPERIMENTAL METHOD	15
3.1 Background Research	15
3.2 Design Blade Turbine	16
3.3 Experimental Setup	18
3.4 Measurements and Instrumentation	19

CHAPTER 4: RESULTS AND DISCUSSIONS	22
4.1 Static Torque of the First New Configuration of Savonius Rotors	22
4.2 Mechanical Power of the First New Configuration of Savonius Rotors	27
4.3 Effect of Models on Static Torque of The First New Configuration of Savonius Rotors	31
4.4 Effect of Models on Mechanical Power of The First New Configuration of Savonius Rotors	34
4.5 Effect of Wind Speed Average Static Torque and Mechanical Power of the First New Configuration of Savonius Rotors	38
4.6 Effect of RPM Average Static Torque and Mechanical Power of the First New Configuration of Savonius Rotors	40
4.7 Static Torque of the Second New Configuration of Savonius Rotors	42
4.8 Mechanical Power of the Second New Configuration of Savonius Rotors	
4.9 Effect of Models on Static Torque of The Second New Configuration of Savonius Rotors	46
4.10 Effect of Models on Mechanical Power of The Second New Configuration of Savonius Rotors	49
4.11 Effect of Wind Speed Average Static Torque and Mechanical Power of the Second New Configuration of Savonius Rotors	53
4.12 Effect of RPM Average Static Torque and Mechanical Power of the Second New Configuration of Savonius Rotors	59
4.13 Comparison between first and second configuration of the rotors	60
CHAPTER 5: CONCLUSIONS AND FUTURE WORKS.....	64
5.1 Conclusions.....	64
5.2 Future Works.....	65
REFERENCES.....	66

LIST OF TABLES

Table 3.1:	Geometric parameters of new design of Savonius turbine	18
Table 4.1:	Models of new design of Savonius wind rotors	22
Table 4.2:	Comparatives average static torque and average mechanical power of the first new configuration of rotors	40
Table 4.3:	Comparatives average static torque and average mechanical power of the second new configuration of rotors	58

LIST OF FIGURES

Figure 2.1:	Components of a horizontal-axis wind turbine	5
Figure 2.2:	A conventional Savonius wind rotor	7
Figure 2.3:	A vertical-axis wind turbine	8
Figure 2.4:	Drag and lift components of the aerodynamic force	9
Figure 2.5:	Models of Savonius rotor	10
Figure 2.6:	Schematic diagram of a different two bladed Savonius rotor	11
Figure 2.7:	Vector components of the wind speed at Savonius rotor	13
Figure 2.8:	Scheme of a Savonius rotor showing the velocity of the rotor and wind speed	14
Figure 3.1:	Configuration of Savonius rotors	16
Figure 3.2:	Geometry of new configurations of Savonius wind turbine	17
Figure 3.3:	Schematic view of experimental setup	19
Figure 3.4:	Procedure for calculating mechanical power of Savonius rotor	21
Figure 4.1:	Static torque vs. angle of rotation for model 1	23
Figure 4.2:	Static torque vs. angle of rotation for model 2	24
Figure 4.3:	Static torque vs. angle of rotation for model 3	24
Figure 4.4:	Static torque vs. angle of rotation for model 4	25
Figure 4.5:	Static torque vs. angle of rotation for model 5	25
Figure 4.6:	Static torque vs. angle of rotation for model 6	26
Figure 4.7:	Static torque vs. angle of rotation for model 7	26
Figure 4.8:	Mechanical power vs. angle of rotation for model 1	27
Figure 4.9:	Mechanical power vs. angle of rotation for model 2	28
Figure 4.10:	Mechanical power vs. angle of rotation for model 3	28
Figure 4.11:	Mechanical power vs. angle of rotation for model 4	29
Figure 4.12:	Mechanical power vs. angle of rotation for model 5	29
Figure 4.13:	Mechanical power vs. angle of rotation for model 6	30
Figure 4.14:	Mechanical power vs. angle of rotation for model 7	30
Figure 4.15:	Static torque vs. rotor angle of first new configuration of rotors at 3 m/s	31

Figure 4.16:	Static torque vs. rotor angle of first new configuration of rotors at 5 m/s	32
Figure 4.17:	Static torque vs. rotor angle of first new configuration of rotors at 7 m/s	32
Figure 4.18:	Static torque vs. rotor angle of first new configuration of rotors at 9 m/s	33
Figure 4.19:	Static torque vs. rotor angle of first new configuration of rotors at 11 m/s	33
Figure 4.20:	Static torque vs. rotor angle of first new configuration of rotors at 13 m/s	34
Figure 4.21:	Mechanical power vs. rotor angle of first new configuration of rotors at 3 m/s	35
Figure 4.22:	Mechanical power vs. rotor angle of first new configuration of rotors at 5 m/s	35
Figure 4.23:	Mechanical power vs. rotor angle of first new configuration of rotors at 7 m/s	36
Figure 4.24:	Mechanical power vs. rotor angle of first new configuration of rotors at 9 m/s	36
Figure 4.25:	Mechanical power vs. rotor angle of first new configuration of rotors at 11 m/s	37
Figure 4.26:	Mechanical power vs. rotor angle of first new configuration of rotors at 13 m/s	37
Figure 4.27:	Average static torque vs. wind speed of first new configuration of rotors	38
Figure 4.28:	Average mechanical power vs. wind speed of first new configuration of rotors	39
Figure 4.29:	Average static torque vs. RPM of first new configuration of rotors ...	41
Figure 4.30:	Average mechanical power vs. RPM of first new configuration of rotors	42
Figure 4.31:	Static torque vs. angle of rotation for model 8	43
Figure 4.32:	Static torque vs. angle of rotation for model 9	43
Figure 4.33:	Static torque vs. angle of rotation for model 10	44
Figure 4.34:	Static torque vs. angle of rotation for model 11	44
Figure 4.35:	Static torque vs. angle of rotation for model 12	45
Figure 4.36:	Static torque vs. angle of rotation for model 13	45

Figure 4.37:	Mechanical power vs. angle of rotation for model 8	46
Figure 4.38:	Mechanical power vs. angle of rotation for model 9	47
Figure 4.39:	Mechanical power vs. angle of rotation for model 10	47
Figure 4.40:	Mechanical power vs. angle of rotation for model 11	48
Figure 4.41:	Mechanical power vs. angle of rotation for model 12	48
Figure 4.42:	Mechanical power vs. angle of rotation for model 13	49
Figure 4.43:	Static toque vs. rotor angle of second configuration of rotors at 3 m/s	50
Figure 4.44:	Static toque vs. rotor angle of second configuration of rotors at 5 m/s	50
Figure 4.45:	Static toque vs. rotor angle of second configuration of rotors at 7 m/s	51
Figure 4.46:	Static toque vs. rotor angle of second configuration of rotors at 9 m/s	51
Figure 4.47:	Static toque vs. rotor angle of second configuration of rotors at 11 m/s	52
Figure 4.48:	Static toque vs. rotor angle of second configuration of rotors at 13 m/s	52
Figure 4.49:	Mechanical power vs. rotor angle of second configuration of rotors at 3 m/s	53
Figure 4.50:	Mechanical power vs. rotor angle of second configuration of rotors at 5 m/s	54
Figure 4.51:	Mechanical power vs. rotor angle of second configuration of rotors at 7 m/s	54
Figure 4.52:	Mechanical power vs. rotor angle of second configuration of rotors at 9 m/s	55
Figure 4.53:	Mechanical power vs. rotor angle of second configuration of rotors at 11 m/s	55
Figure 4.54:	Mechanical power vs. rotor angle of second configuration of rotors at 13 m/s	56
Figure 4.55:	Average static torque vs. wind speed of second new configuration of rotors	57
Figure 4.56:	Average mechanical power vs. wind speed of second new configuration of rotors	57

Figure 4.57:	Average static torque vs. RPM of second new configuration of rotors	59
Figure 4.58:	Average mechanical power vs. RPM of second new configuration of rotors	60
Figure 4.59:	Comparison static torque and mechanical power of model 1, 2 and 8	61
Figure 4.60:	Comparison static torque and mechanical power of model 1, 3 and 9	61
Figure 4.61:	Comparison static torque and mechanical power of model 1, 4 and 10	62
Figure 4.62:	Comparison static torque and mechanical power of model 1, 5 and 11	62
Figure 4.63:	Comparison static torque and mechanical power of model 1, 6 and 12	63
Figure 4.64:	Comparison static torque and mechanical power of model 1, 7 and 13	63

LIST OF SYMBOLS USED

A	Swept area, m ²
C_D	Drag coefficient
C_L	Lift coefficient
C_P	Power coefficient
C_T	Torque coefficient
F_D	Drag force, N
F_L	Lift force, N
n	Rotational speed in revolutions per second, RPM
P_m	Mechanical power, W
$P_{m,average}$	Average mechanical power, W
v_{rotor}	Rotor velocity, m/s
v_{rel}	Relative velocity, m/s
v_{wind}	Wind velocity, m/s
T	Actual torque, N.m
$T_{average}$	Average static torque, N.m
ω	Angular velocity, rad/s
ρ	Air density, kg/m ³

CHAPTER 1

INTRODUCTION

1.1 Background

Wind energy is a renewable and clean energy resource. One of the wind turbines of vertical axis, Savonius rotor (Sayigh, 2015) is a drag type. The performance of Savonius rotor is lower than other types of vertical axis wind turbine. For example, the configuration of Savonius rotor design is simple and cheap (Sayigh, 2015). They start to run on their own and they are independent of the direction of the wind (Prenis, 1977). They also have a high starting torque (Turner, 2005; Sun et al., 2016). Despite such a certain number of advantages of Savonius wind rotors; they are not preferred so much due to their low aerodynamic performance levels. To reduce this disadvantageous quality of Savonius wind rotors, numerous studies experimentally and numerically have been done in order to increase the efficiency of Savonius rotors (Driss et al., 2014). Consequently, this research presents an experimental study of small scale new configuration of Savonius vertical axis wind turbines having multiple halves blades. In addition, it describes the effect of some design parameters including wind speed, rotor position, halves blade height, and location of halves blades on the performance of them.

1.2 Research Goals

The aim of this thesis is to investigate the effect of halves blades and their geometries on the performance of new configuration of Savonius vertical axis wind turbine having multiple halves blades. Therefore, the specific objectives of this work are:

1. Study the characteristic of static torque and mechanical power of new configuration of Savonius rotors in low wind speed conditions.
2. Study the impact of halves blade geometries on the mechanical power of the rotors at different rotor positions and wind speed.
3. Compare the mechanical power of new configuration Savonius rotors with conventional Savonius rotors.

1.3 Research Outline

This chapter presents a brief introduction to wind power and its significance for human life. In chapter 2, wind turbine background is explained in details, followed by history of wind turbine and discussion of the type of turbines, which are the major topic of this work. Chapter 3 demonstrates the designed and method for measuring the static torque and mechanical power of the rotors. All the results of the experiments are presented in chapter 4 for new configuration of Savonius rotors. The thesis ends with conclusions and suggestions for future work in chapter 5.

CHAPTER 2

WIND TURBINE FUNDAMENTAL

This chapter briefly discusses the history of wind turbine and types of wind turbine. Furthermore, it permanently explained the type of vertical axis wind turbine, and their advantage and application.

2.1 History of Wind Turbines

Wind machines were used for grinding grain in Persia as early as 200 B.C. In Denmark, by 1900, about 2500 windmills were used to produce more than 30 MW.

The first windmill for electricity production was built by Charles F Brush in 1888, and in 1908 there were 72 wind-driven electric generators from 5 kW to 25 kW. The largest machines were on 24 m (79 ft) towers with four-bladed 23 m (75 ft) diameter rotors. At the time of the First World War, 100,000 farm windmills were produced every year by the Americans, most of it were used to run water pumps. By the 1930s it was common to utilize windmills for electricity generation in farms as most of it the United States did not have the distribution systems (Lange and Grant 1995).

The beginning of the electricity generating windmill operated in the UK was a battery charging machine made by James Blyth and installed in 1887 in Scotland. In 1954 John Brown Company made the first utility grid-connected wind turbine operated in the UK. It was about 18 meter in diameter, three bladed and gives a rated output power of 100 kW (Lange and Grant 1995).

2.2 Turbine Classification

Wind turbines can be separated into two types based on the axis on which the turbine rotates. Turbines that rotate around a horizontal axis, known as Horizontal Axis Wind Turbine (HAWT) are more common than Vertical-Axis Wind Turbines (VAWT) that rotate around a vertical axis (Steeby, 2012).

2.2.1 Horizontal Axis Wind Turbines

Horizontal-axis wind turbines (HAWT) have its rotating shaft fixed horizontally with high tower to utilize high wind speeds (Magedi et al., 2014). Small turbines are pointed by a

simple wind vane, while large turbines generally use a wind sensor coupled with a servo motor. Most of the horizontal-axis wind turbines have a gear box to control the shaft speed and turns the slow rotation of the blades into a quicker rotation that is more suitable to drive a generator (Soliman, 2011; Tong, 2010). The principal subsystems of a typical horizontal-axis wind turbine as shown in Figure 2.1 include (Manwell et al., 2011)

- The rotor, consisting of the blades and the supporting hub
- The power train, which includes the rotating parts of the wind turbine (exclusive of the rotor); it usually consists of shafts, gearbox, coupling, a mechanical brake and the generator
- The nacelle structure and main frame; including wind turbine housing, bedplate and the yaw system
- The tower and the foundation
- The machine controls
- The balance of the electrical system, including cables, switchgear, transformers and possibly electronic power converters

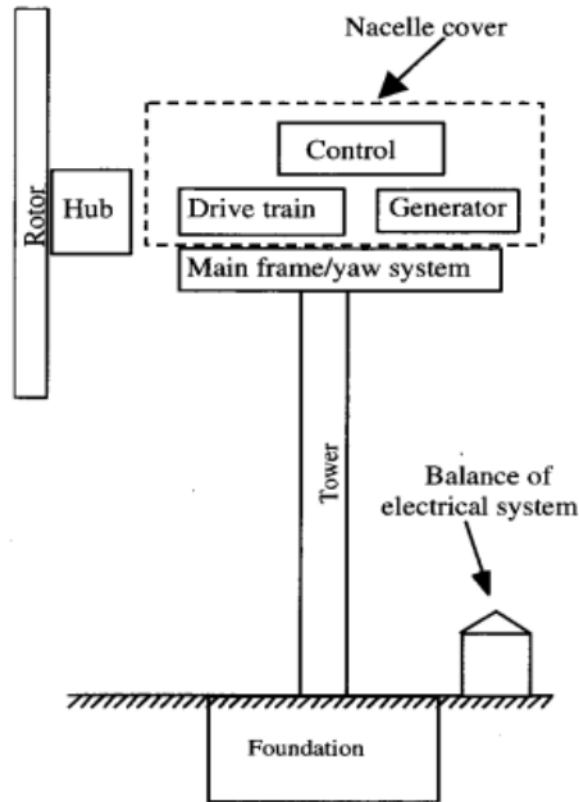


Figure 2.1: Components of a horizontal-axis wind turbine (Manwell et al., 2011)

A gear box is used to control the angular speed of the generator to be able to get a constant output power at different air speeds; there are also designs that use direct drive of an annular generator (Castellano, 2012). Some models operate at constant speed, but more energy can be collected by variable-speed turbines which use a solid-state power converter to interface to the transmission system. All turbines have a safety system which shut down the turbine if it was running over the designed speed or when the vibrations exceed the safe range (Hau & Hau, 2006).

2.2.2 Vertical Axis Wind Turbines

The rotor of this wind machine rotates perpendicular to the direction of the wind (Ledec et al., 2011).. It has some advantages over the VAWTs, these include its simple construction, its ability to catch the wind from any direction and high starting torque (Savonius rotor).

However, this machine has also some disadvantages such as low power coefficient compared to that of the HAWTs, and poor starting torque (Darrieus rotor). . It also does not need a high tower which makes it much cheaper than the horizontal-axis wind turbine (Paraschivoiu, 2002).

Normally VAWTs can be divided into two main types:

- Drag type like Savonius rotor or S-rotor
- Lift type such as Darrieus rotor or D-rotor

2.2.2.1 Savonius rotor

Savonius wind rotor is a vertical-axis wind turbine made-up by the Finnish engineer Sigurd Savonius in 1925. A conventional Savonius wind rotor is consisted of two semi-cylinders called blades, which are placed in between two horizontal discs and the centers of which are symmetrically sided. When the moment on the convex blade of the Savonius wind rotor is compared with the moment on the concave blade, it seems that the former is lower because of the different resistance coefficients of the surfaces. For this reason, the Savonius wind rotor rotates in the direction of the positive moment that forms on the concave blade. The Savonius turbine mainly depends on the drag force resulting from the wind due to the curvature sides. Below is a simple figure for the running principle of the Savonius wind rotor (Figure 2.2). It is economical for the small power requirements, and it generates a high starting torque but has a lower power coefficient of about 0.25 (Lissaman & Willson, 1974; Le, 2014). At its most basic level, an S-rotor comprises two half cylinders displaced so that one convex face and one concave face are presented to the wind (Figure 2.2). The difference in drag on two sides produces a torque for most, but not all, orientations to the wind. Therefore, at least two rotors at different angles are required to ensure self-starting.

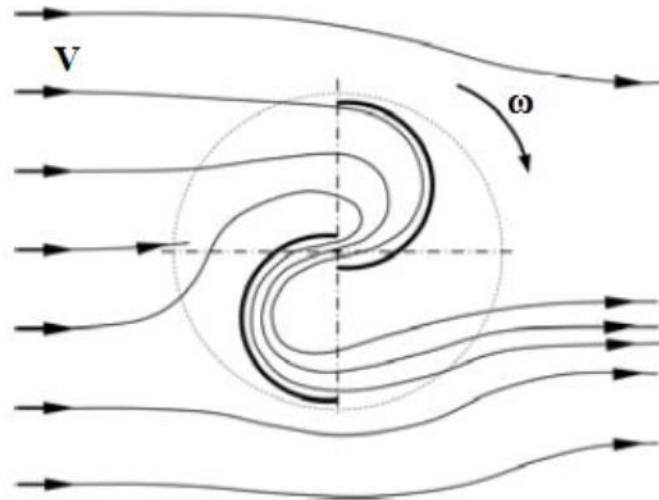


Figure 2.2: A conventional Savonius wind rotor (Altan & Atılgan, 2012)

2.2.2.2 Darrieus Wind Turbine

Georges Darrieus of Paris filed a United States patent in 1926 for vertical axis rotor (Lissaman & Willson, 1974) as shown in Figure 2.3. These kinds of turbines have good efficiency, but they produce high stresses over the turbines blades and the tower making no reliable. They need also an external motor to initiate the rotating at the beginning because the starting torque is very low. The torque ripple is reduced by using 3 or more blades which results in a higher solidity for the rotor. The blade solidity is measured by blade area over the rotor area (Peace, 2004).

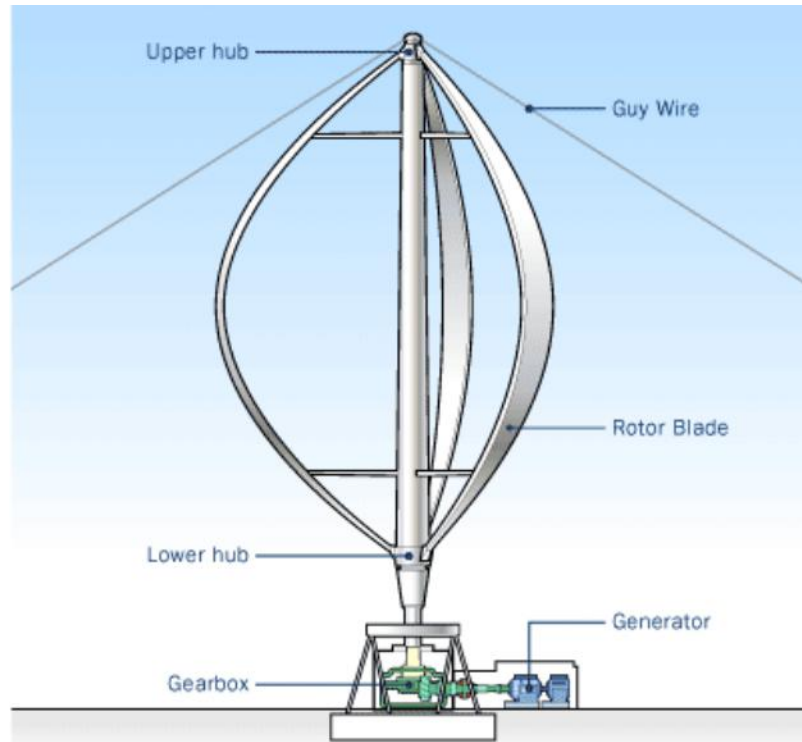


Figure 2.3: A vertical-axis wind turbine ((Paraschivoiu, 2002)

2.3 VAWT Advantages and Applications

1. It is easy to maintain because it is close to the ground.
2. VAWTs have a higher airfoil pitch angle, giving improved aerodynamics while decreasing drag at low and high pressures (Sharma & Kar, 2015).
3. Straight bladed VAWT designs with a square or rectangular cross section has a larger swept area for a given diameter than the circular swept area of HAWTs.
4. Low height is useful where laws do not permit structures to be placed high.
5. It does not need a high standing tower because it works efficiently at lower wind speeds which can be obtained near of the ground.
6. They have a lower Tip-Speed ratio so it will be stronger and last longer than HAWT.
7. It is a self oriented turbine, it does not need to face the wind to rotate, and it catches the wind from any direction.

8. They can potentially be built to a far larger size than HAWT's , for instance floating VAWT's hundreds of meters in diameter where the entire vessel rotates , can eliminate the need for a large and expensive bearing.
9. There may be a height limitation to how tall a vertical wind turbine can be built and how much swept area it can have. However, this can be overcome by connecting a multiple number of turbines together in a triangular pattern with bracing across the top of the structure, thus reducing the need for such strong vertical support, and allowing the turbine blades to be made much longer (Jha, 2011; Chiras et al., 2010).

2.5 Drag type and lift type wind turbines

When a flat object is exposed to an incident wind, it encounters a surface force, commonly known as aerodynamics force (Figure 2.4) The component of the aerodynamic force that is parallel to the flow direction is called drag while the one, perpendicular to the direction of wind, is called lift (Da, 2005). Magnitude of the drag force and the lift force are determined by following expressions:

$$F_D = \frac{1}{2} \rho V^2 C_D A \quad (2.1)$$

$$F_L = \frac{1}{2} \rho V^2 C_L A \quad (2.2)$$

where A is the planform area (projected area perpendicular to the flow velocity) of the object, ρ is density of the air, and V is the upstream wind speed and, C_D and C_L are proportional constants called drag and lift coefficients respectively. The constants depend on the 'aerodynamic quality of the object: the better the aerodynamic quality of the object, the higher C_L is the lift coefficient but lower C_D is the drag coefficient, and thus higher the lift force but lower drag force.

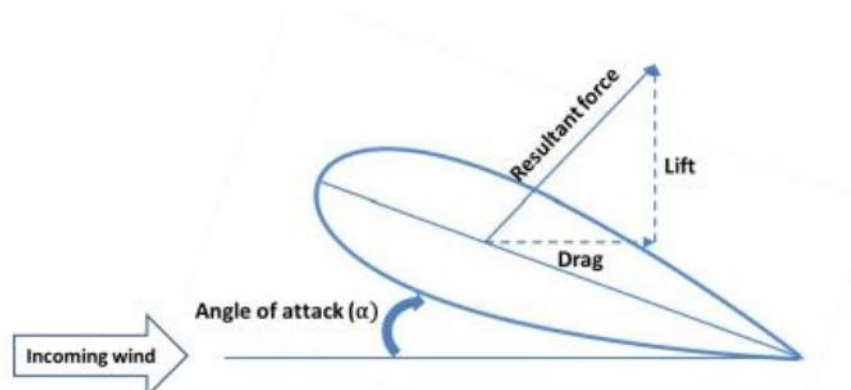


Figure 2.4: Drag and Lift components of the aerodynamic force (Kishore, 2013)

As discussed earlier, the Savonius type rotor is a drag-based wind turbine because it's the drag component of the aerodynamic force that powers the Savonius turbine to rotate. There are two basic models of Savonius wind turbine rotor (without and with overlap or gap) (Rogowski & Maroński, 2015) as shown in Figure 2.5.

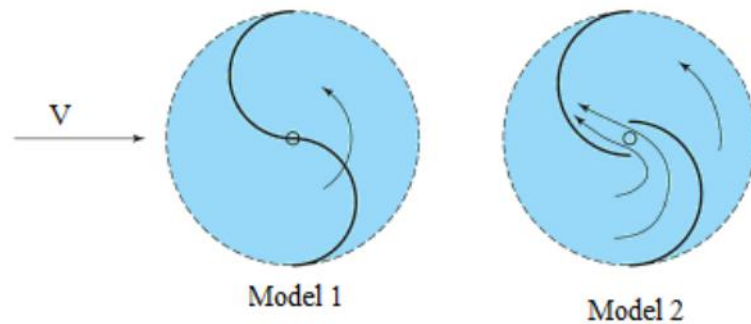


Figure 2.5: Models of Savonius rotor

We can estimate the torque, and mechanical power output of a Savonius rotor using a simplified model, Figure 2.6. This simplified model, however neglects the effect of rotor on the wind flow characteristics (Kishore, 2013).

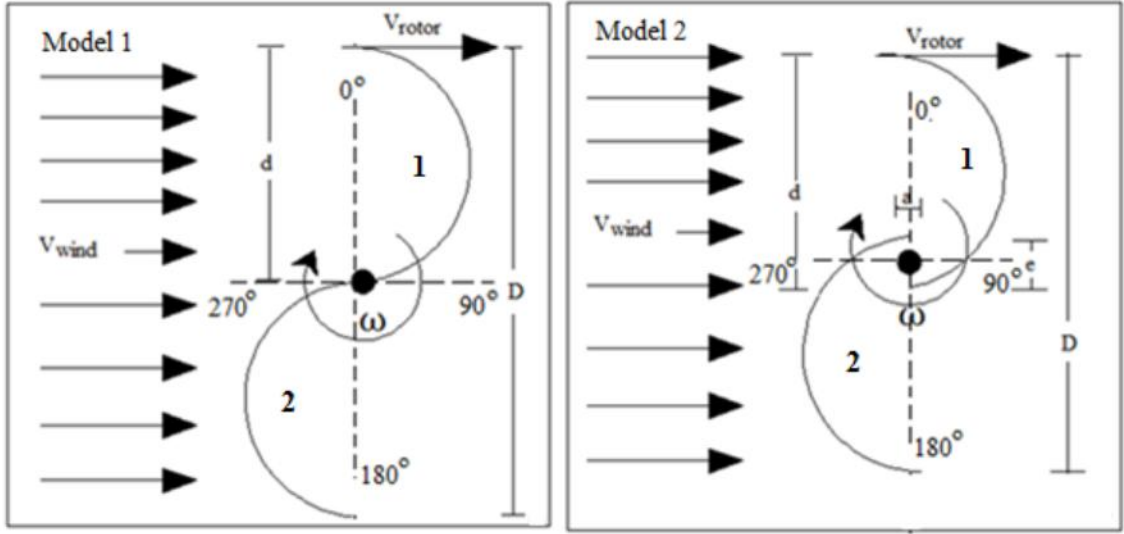


Figure 2.6: Schematic diagram of a different two bladed Savonius rotor

Let's assume that the rotor has mean radius R and it is rotating with an angular speed ω . The circumferential velocity of the rotor or rotor velocity, v_r , at the mean radius is equal to:

$$v_{rotor} = \omega R \quad (2.3)$$

during the rotation, the wind velocity is broken into two components: X, and Y as shown in Figure 2.7. Vertical flows were not considered in this research, and could be a topic for future exploration. Assuming that the axis of the C-section vertical axis wind turbine rotor is the upward-pointing Y-axis, the flow experienced in the X-direction is the sum of the free-stream flow in the X-direction, and the X-aspect of rotational velocity (see Figure 2.8).

Let assume that the rotor is rotating (see Figure 2.6), then the average relative velocities of the wind $v_{rel,1}$ and $v_{rel,2}$ at the first and second rotating drums are given by following expressions, respectively (see Figure 2.8).

$$v_{rel,1} = V \cos\theta - v_{rotor} \quad (2.4)$$

$$v_{rel,2} = V \cos\theta + v_{rotor} \quad (2.5)$$

The average relative velocities of the wind $v_{rel,1}$ and $v_{rel,2}$ at the first and second rotating buckets depend on the rotor position. Therefore, as mention previously, during the rotation

the wind velocity is broken into two components term of sine or cosine as shown in Figure 2.7 and Equations 2.4 to 2.7.

The resulting drags forces $F_{D,1}$ and $F_{D,2}$ on the rotating drums (Kishore, 2013) are given as:

$$\begin{aligned} F_{D,1} &= \frac{1}{2} \rho C_{D,1} v_{rel,1}^2 A = \frac{1}{2} \rho C_{D,1} A (V - v_{rotor})^2 \\ &= \frac{1}{2} \rho C_{D,1} A V^2 \left(\cos\theta - \frac{v_{rotor}}{V} \right)^2 \end{aligned} \quad (2.8)$$

$$\begin{aligned} F_{D,2} &= \frac{1}{2} \rho C_{D,2} v_{rel,2}^2 A = \frac{1}{2} \rho C_{D,2} A (V + v_{rotor})^2 \\ &= \frac{1}{2} \rho C_{D,2} A V^2 \left(\cos\theta + \frac{v_{rotor}}{V} \right)^2 \end{aligned} \quad (2.9)$$

where, A denotes projected area of the drums. The aerodynamic torque along the central axis is calculated as (Kishore, 2013):

$$\begin{aligned} T &= (F_{D,1} - F_{D,2}) \left(\frac{D}{2} \right) \\ &= \frac{1}{2} \rho A V^2 \left[C_{D,1} \left(\cos\theta - \frac{v_{rotor}}{V} \right)^2 \right. \\ &\quad \left. - C_{D,2} \left(\cos\theta + \frac{v_{rotor}}{V} \right)^2 \right] \left(\frac{D}{2} \right) \end{aligned} \quad (2.10)$$

The mechanical power by the turbine can be then determined using the following equation (Kishore, 2013).

$$\begin{aligned} PM &= T\omega = \frac{1}{2} \rho A V^2 \left[C_{D,1} \left(\cos\theta - \frac{v_{rotor}}{V} \right)^2 - C_{D,2} \left(\cos\theta + \frac{v_{rotor}}{V} \right)^2 \right] \omega \left(\frac{D}{2} \right) \\ &= \frac{1}{2} \rho C_p v_{wind}^3 A \end{aligned} \quad (2.11)$$

The expression $\left[C_{D,1} \left(\cos\theta - \frac{v_{rotor}}{V} \right)^2 - C_{D,2} \left(\cos\theta + \frac{v_{rotor}}{V} \right)^2 \right]$ is defined as power coefficient, C_p . It can be noted from equation (2.9) that the mechanical power produced by a Savonius turbine is directly proportion to the total projected area by the rotor and the cube of upstream wind speed V. Darrieus VAWTs and HAWTs are the lift-based wind turbines i.e. they extract power from the wind by utilizing mainly the lift component of the aerodynamic force on their blades. The analytical model to predict the power by a Darrieus wind turbine is quite complex (Kishore, 2013).

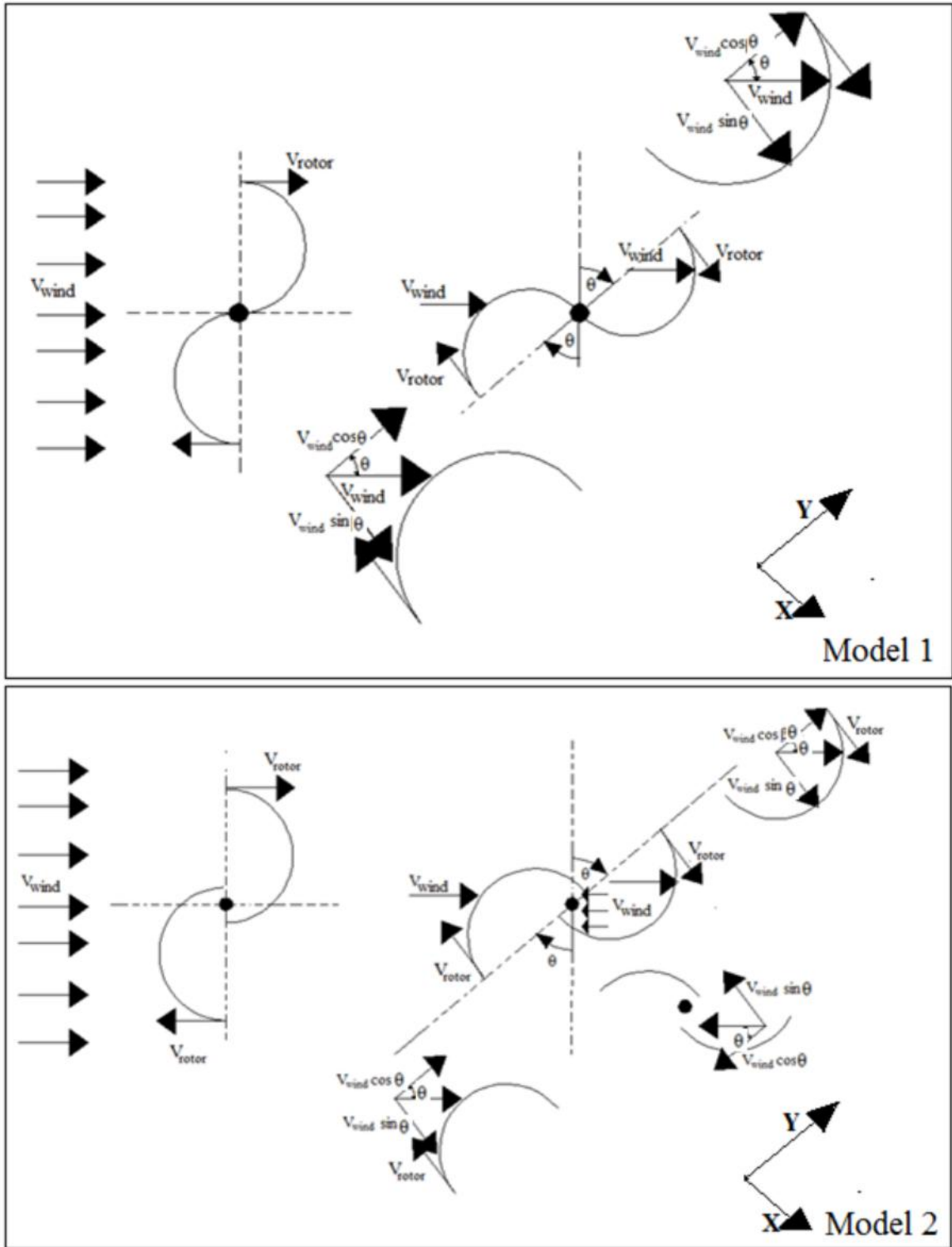


Figure 2.7: Vector components of the wind speed at Savonius rotor

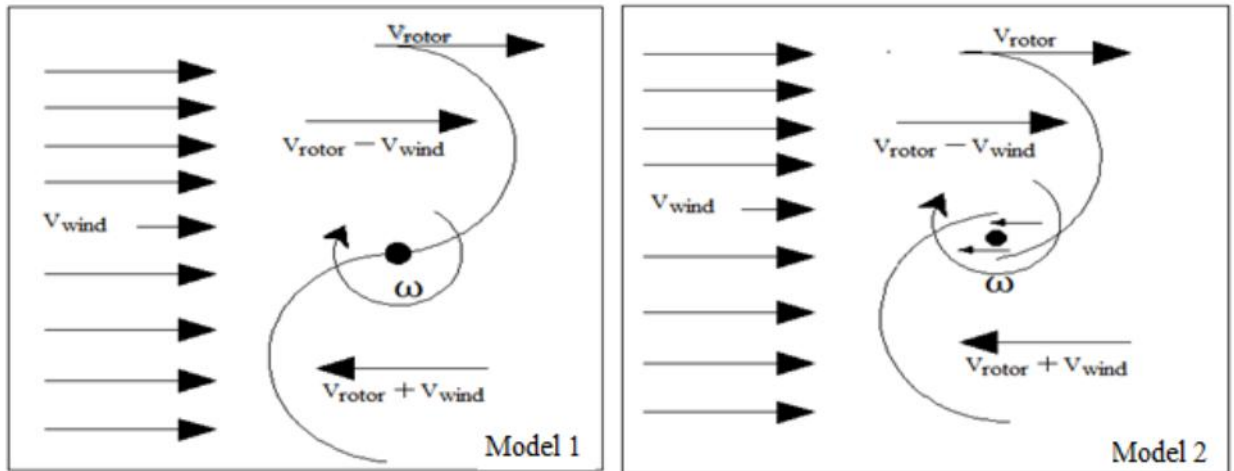


Figure 2.8: Scheme of a Savonius rotor showing the velocity of the rotor and wind speed

CHAPTER 3

EXPERIMENTAL METHOD

In the current study, a comparison is carried out between two different configurations of Savonius having multiple halves blades rotor which are

1. Conventional Savonius rotor
2. New configuration Savonius rotor

To carry out this goal, the objectives were

- 1) Analyze the effect of turbine geometry on the power output
- 2) Analyze the effect of wind speed on the power output

To meet these objectives, the tasks were to:

- Complete with background research on unconventional Savonius wind rotors,
- Design turbine blade designs for testing, and
- Create an experimental setup.

3.1 Background Research

Background research included reviewing a previous research, enclosed unconventional Savonius wind rotor by Sharma & Sharma (2016). The authors studied numerically on the evaluation and comparison of the performance of a new configuration of Savonius rotors having multiple quarter blades with the conventional one. New configuration comprises multiple quarter blades added to conventional configuration as shown in Figure 3.1. In this research, new configuration comprises multiple half blades added to conventional configuration with various geometries were discussed in this chapter.

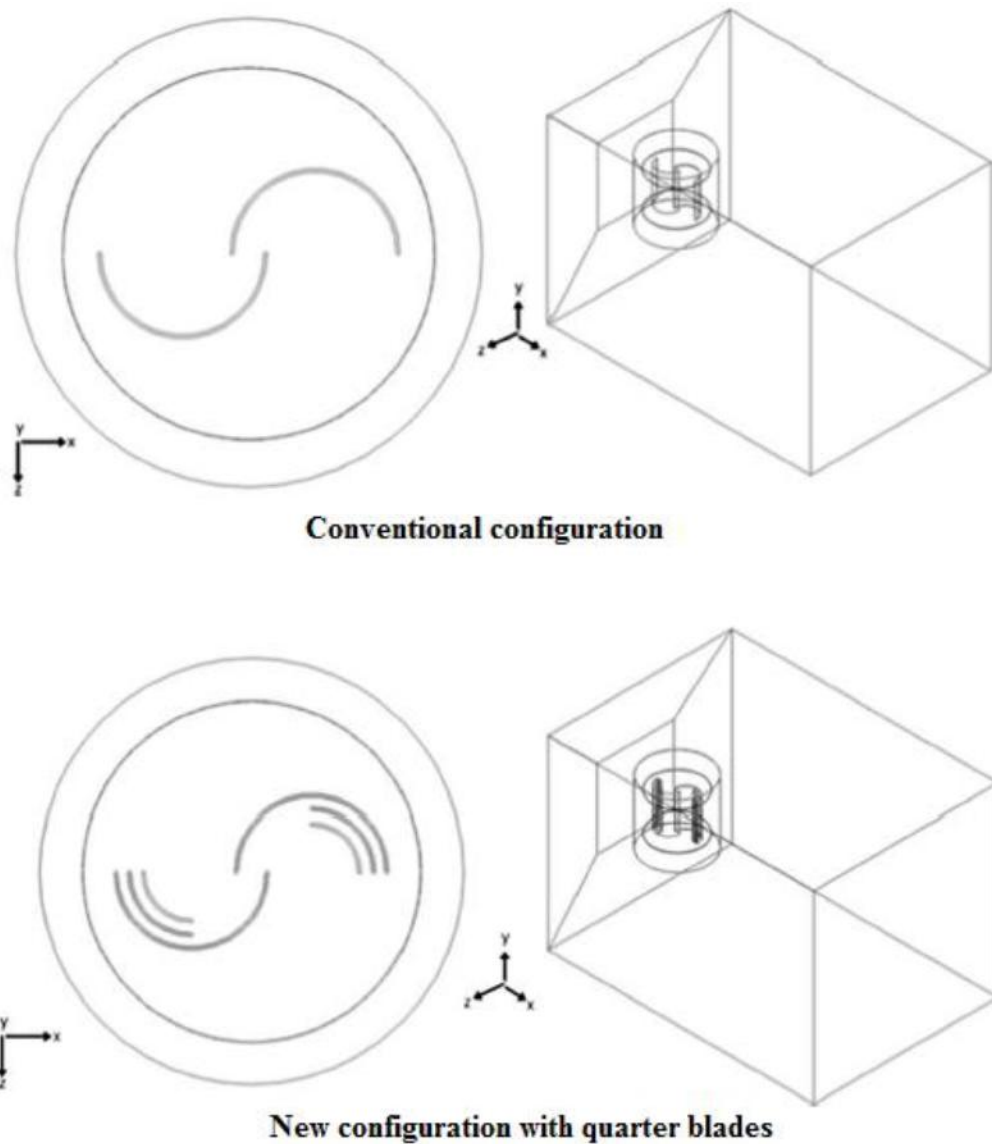


Figure 3.1: Configuration of Savonius rotors (Sharma & Sharma, 2016)

3.2 Design Blade Turbine

The design of blade of turbine usually starts with the definition of the desired or required characteristics. The selection of blade for a wind turbine depends mainly on the lift and drag characteristics of the blade and on the geometry of the blade. During this study, static torque and mechanical power were measured experimentally. This study aims to investigate the effect of new configuration on the performance of a Savonius wind turbine.

The models of a new configuration of Savonius wind turbine blades are shown in Figure 3.2. The dimensions of the rotor models are shown in Table 3.1 and Figure 3.2

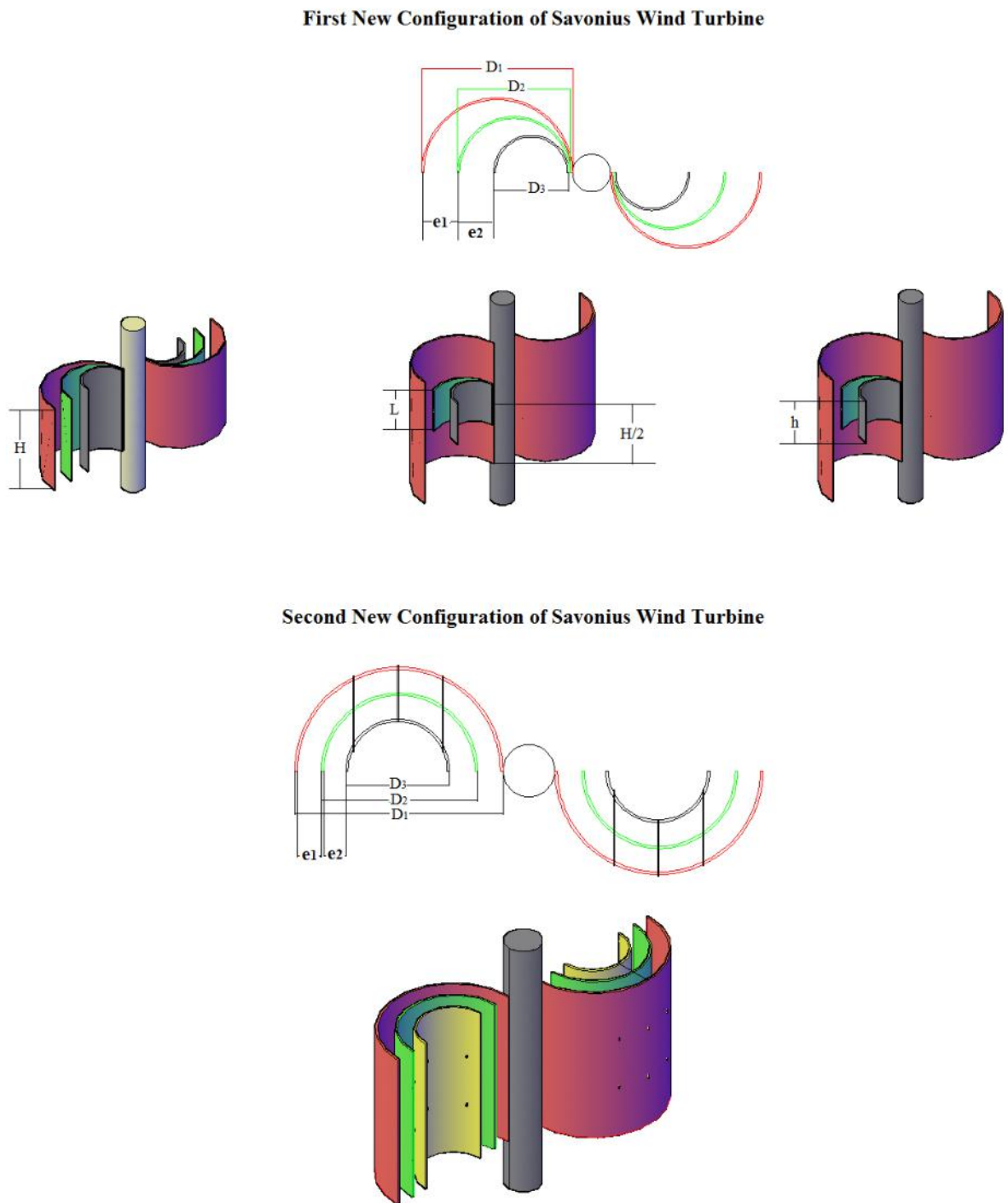


Figure 3.2: Geometry of new configurations of Savonius wind turbine

Table 3.1: Geometric parameters of new design of Savonius turbine

Design parameter	Value
1. D_1	160 mm
2. D_2	$D_2 = D_1 - 20$
3. D_3	$D_3 = D_2 - 20$
4. H	600 mm
5. L	200, 300, 400 mm
6. h	200, 300, 400 mm
7. e_1	4 mm
8. e_2	3 mm
9. Shaft diameter	20mm

3.3 Experimental Setup

The experimental setup in the study was made according to previous study (Mahmoud et al., 2012; Kamoji et al., 2009). Figure 3.3 shows a representation diagram of the experimental set-up used in this work. As can be seen, the experimental set-up consists of three main parts which are the wind tunnel, rotor and measurement devices. The wind tunnel used in the experiments is an open-circuit type and has a squared exit (800 mm \times 800 mm). Its wind velocity could also be changed with the use of an adjustable damper. The Savonius wind rotor and measurement devices have been installed away from the exit of this wind tunnel. Materials were selected to avoid structural failure of the wind turbine due to the forces that winds would impose on the blades. The drive shaft carried the most stress in this system due to the torsion produced by the blades. The Savonius rotor has been placed on a wood table. The shaft was made from galvanized steel. The blade rotors were made of PVC. Two ball bearings have been used to support the rotor shaft at top and bottom and to minimize the friction force. And then measurements of RPM, and wind velocity have been measured by RPM reader and pitot tube, respectively. Additionally, a centrifugal fan is used as the wind source for doing experiments. The wind velocity, V , was set at 3, 5, 7, 9, 11 and 13 m/s by adjusting the distance between the wind tunnel and the structure as shown in Figure 3.3.

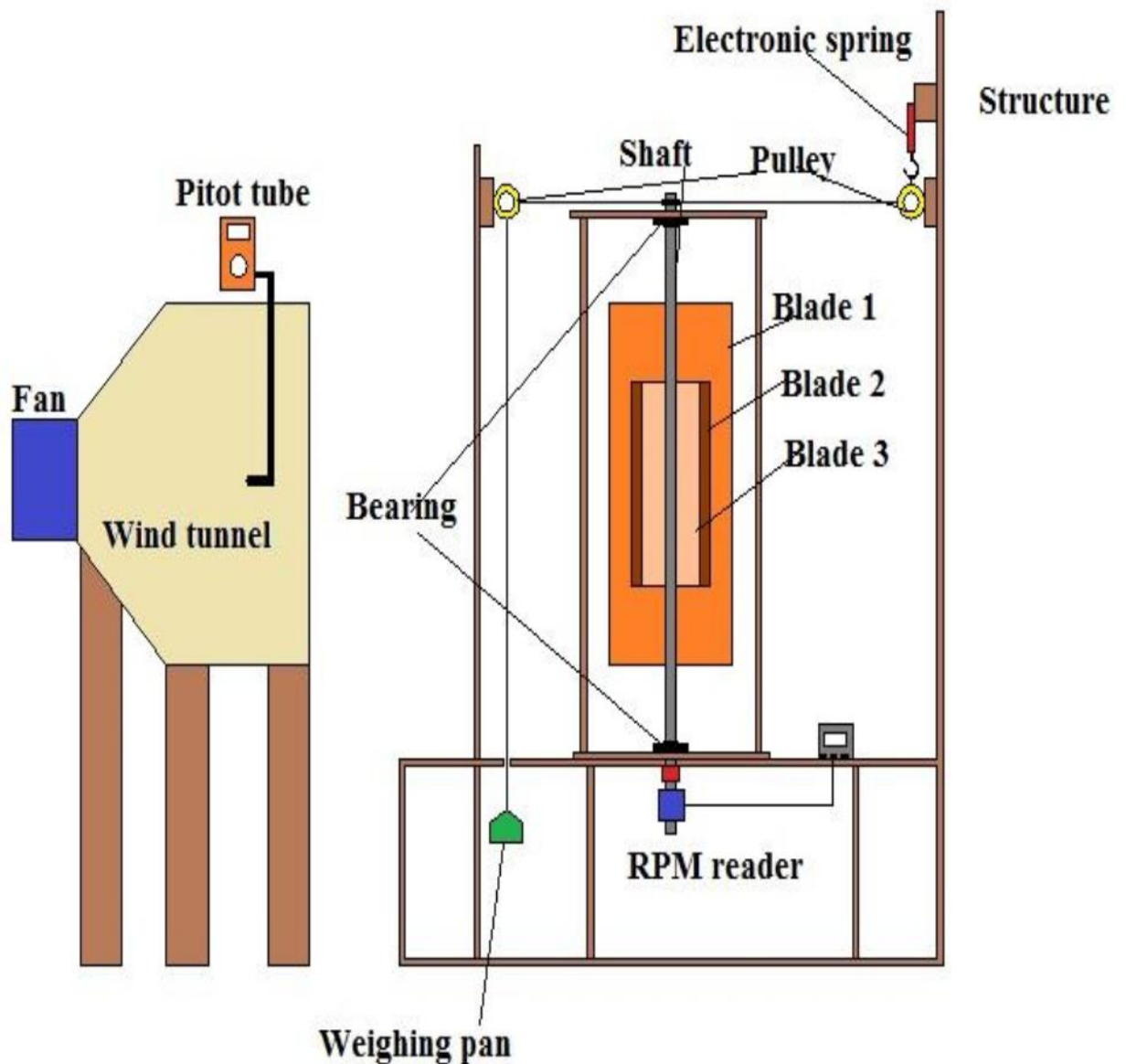


Figure 3.3: Schematic view of experimental setup

3.4 Measurements and Instrumentation

The mechanical power for unconventional Savonius rotors is estimated by multiplying the torque with angular speed at various wind speed and rotor positions. The arrangement used to do that is shown in Figure 3.3. It contains pulley system, nylon string, weighing pan and spring balance. The weighing pan, pulley and spring balance are connected by a nylon

string of 1 mm diameter as shown in Figure 3.3. Pitot tube and RPM reader are used to measure the wind speed and rotational speed of the shaft, respectively. The rotor is loaded gradually to record spring balance reading, weights and rotational speed of the rotor. A set of tests are carried to calculate the static torque and mechanical power of the rotor at a given rotor angle using the brake drum measuring system. The static torque of the rotor is estimated at every 30° of the rotor angle. At a known wind velocity, the rotor is loaded to stop it from rotation at a given angle of rotor. The values of load and spring balance reading are recorded to calculate the static torque at a certain rotor angle

The mechanical power can be determined for each wind speed and rotor position as follow

$$P_m = T\omega \quad (3.1)$$

where T is the torque and ω is the angular speed. The angular speed is defined in rad/s as:

$$\omega = \frac{2\pi n}{60} \quad (3.2)$$

where n is the shaft rotational speed in rpm. The mechanical torque is obtained in (N.m) by

$$T = Fr \quad (3.3)$$

where r is the shaft radius.

The force acting on the rotor shaft obtained in (N) by:

$$F = (m - s)g \quad (3.4)$$

where m is the mass loaded on the pan in kg, s is the spring balance reading in kg and g is the gravitational acceleration.

The procedures of torque and power calculation of unconventional Savonius vertical axis wind turbine can be described in Figure 3.4:

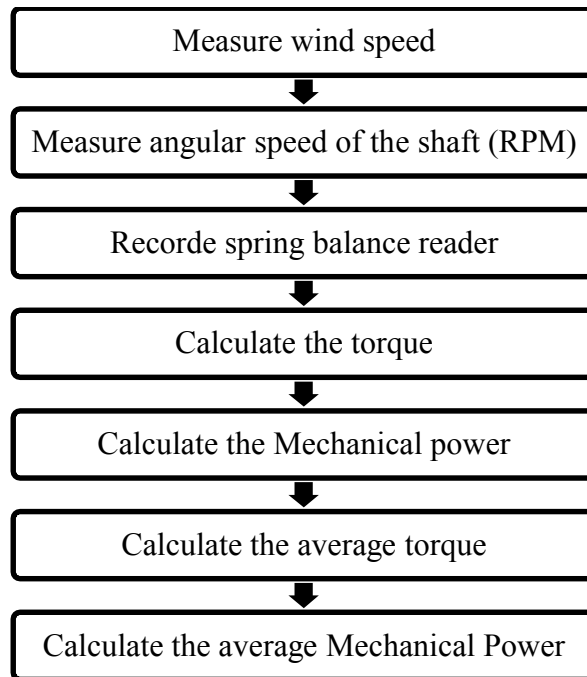


Figure 3.4 Procedure for calculating mechanical power of Savonius rotor

CHAPTER 4

RESULTS AND DISCUSSIONS

Experimental results of static torque which is directly measured and mechanical power along with wind speed is discussed for different design. Finally comparison of static torque and mechanical power are discussed for different models as shown in Table 41.

Table 4.1: Models of new design of Savonius wind rotors

	Models	H [mm]	L [mm]	h [mm]	
Conventional Rotor	Model 1	600	-	-	
	Model 2	600	200	200	
	First configuration of Savonius rotors	Model 3	600	300	300
	Model 4	600	400	400	
	Model 5	600	400	200	
	Model 6	600	400	300	
	Model 7	600	300	200	
Second configuration of Savonius rotors	Model 8	600	200	200	
	Model 9	600	300	300	
	Model 10	600	400	400	
	Model 11	600	400	200	
	Model 12	600	400	300	
	Model 13	600	300	200	

4.1 Static Torque of the Rotors of the First New Configuration of Savonius Rotors

Figures 4.1 to 4.7 show the static torque varies with the change in rotor angle for a different number of wind speed (3, 5, 7, 9, 11, and 13 m/s) and models (see Table 4.1). It can be observed that the static torque is rapidly increasing with the increase in wind speed.

It can be noticed from these figures that the static torque and mechanical power of the new configuration of Savonius wind rotors start to increase from (0° to 60°) to reach its maximum value. The reason is that the inner blades is located completely in front of the flow at 60° and its aerodynamics condition is suitable. Furthermore, from 60° to 120° the torque decreases to reach its lowest value. The static torque values increased slightly from (120° to 240°) to get to the peak value. From 240° to 360° the static torque is fluctuated (Figures 4.1 to 4.6). Additionally, it observed that model 1 has minimum static torque than other models. Moreover, the blade heights of the halves blades directly affect the static torque of the rotors as shown in the Figures 4.1 to 4.7. Consequently, the distance (e) between the blades (see Figure 3.2) of can be considered as an important factor that has great influence on the torque output of the rotor. In addition, the difference of halves blade height is another factor that effect on the static torque output i.e. when the difference between the inner halves blades and the outer halves blades increases, the acting force on the rotors is increasing rapidly, which leads to increase the static torque output. Another factor may be effect on the static torque output is weight of the rotors. As mention in chapter 3, static torque is a force exerted at a distance (shaft radius) from the axis of rotation i.e. variation between mass loaded and spring balance reader leads to increase or decrease the force acting on the rotors.

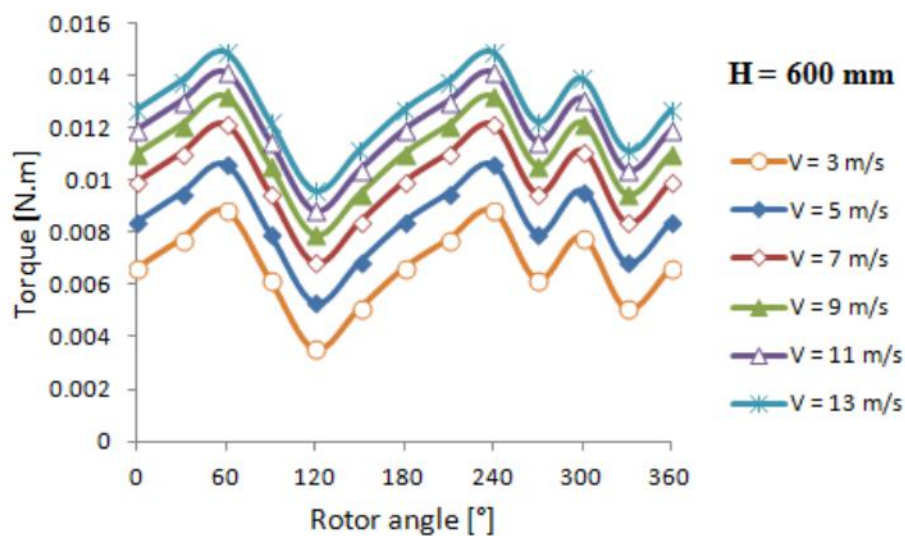


Figure 4.1: Static torque vs. angle of rotation for model 1

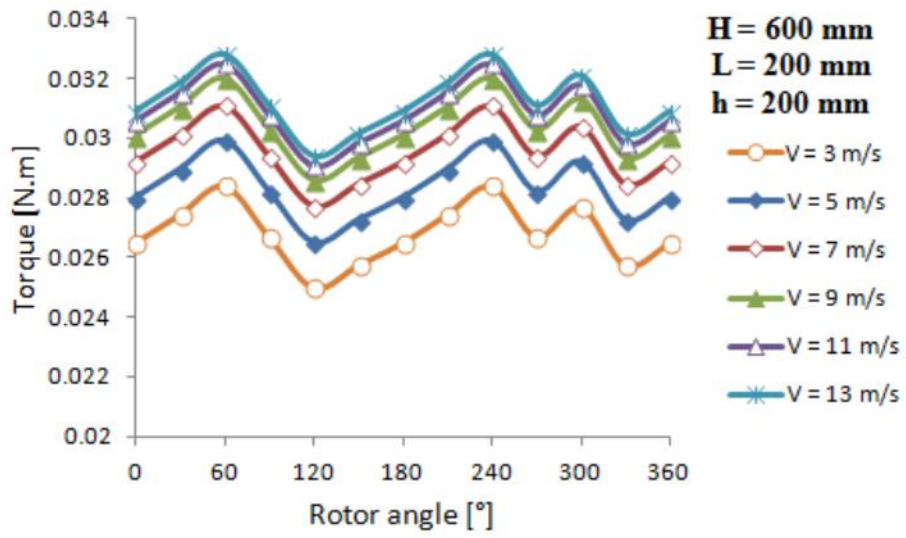


Figure 4.2: Static torque vs. angle of rotation for model 2

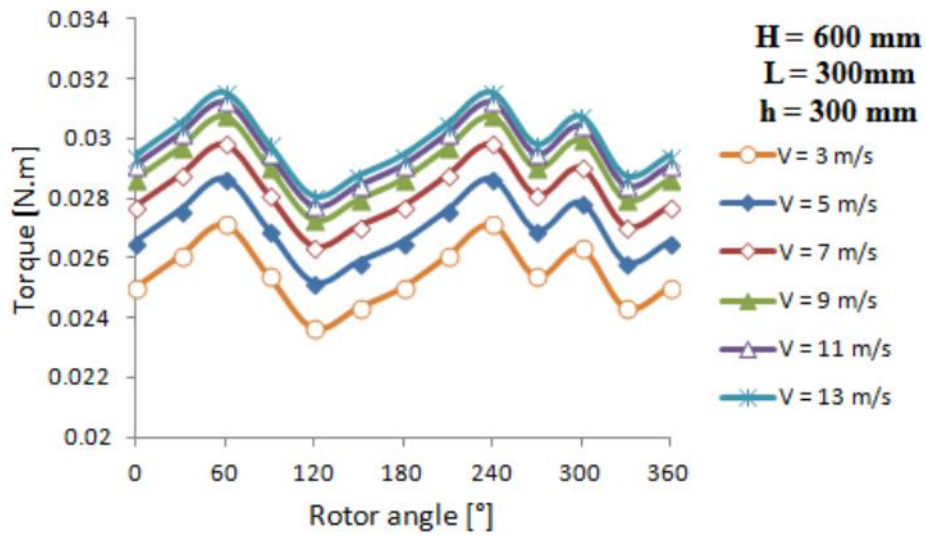


Figure 4.3: Static torque vs. angle of rotation for model 3

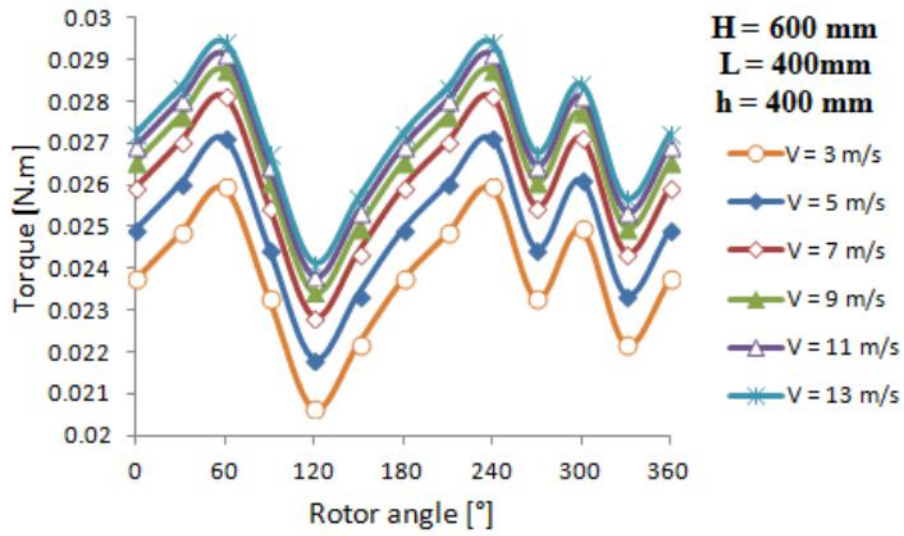


Figure 4.4: Static torque vs. angle of rotation for model 4

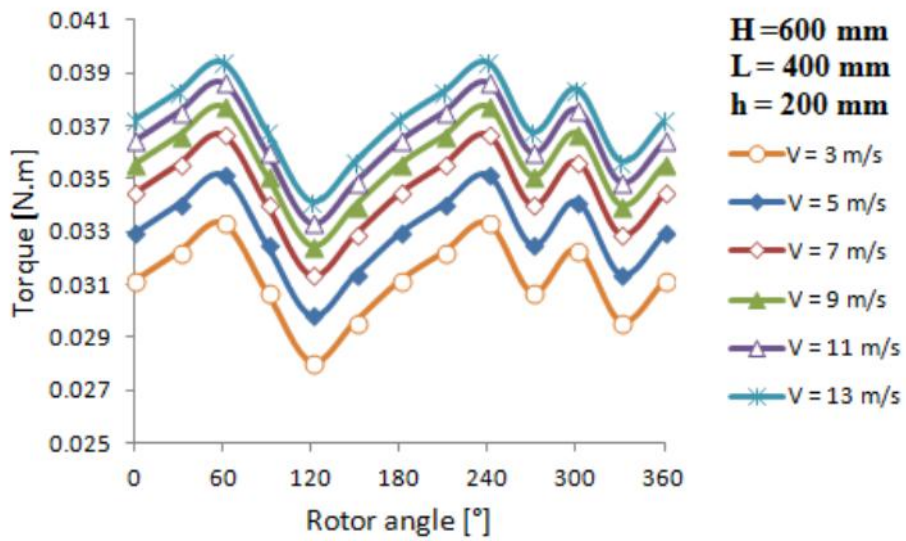


Figure 4.5: Static torque vs. angle of rotation for model 5

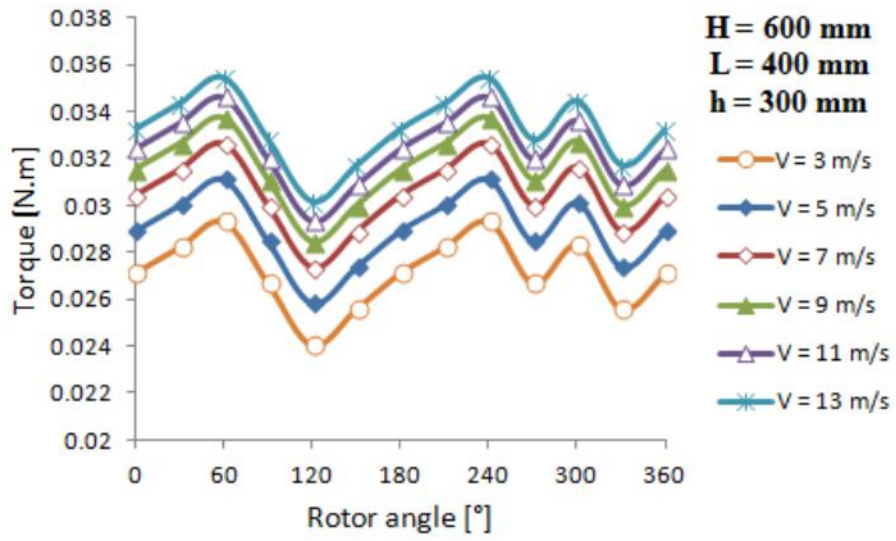


Figure 4.6: Static torque vs. angle of rotation for model 6

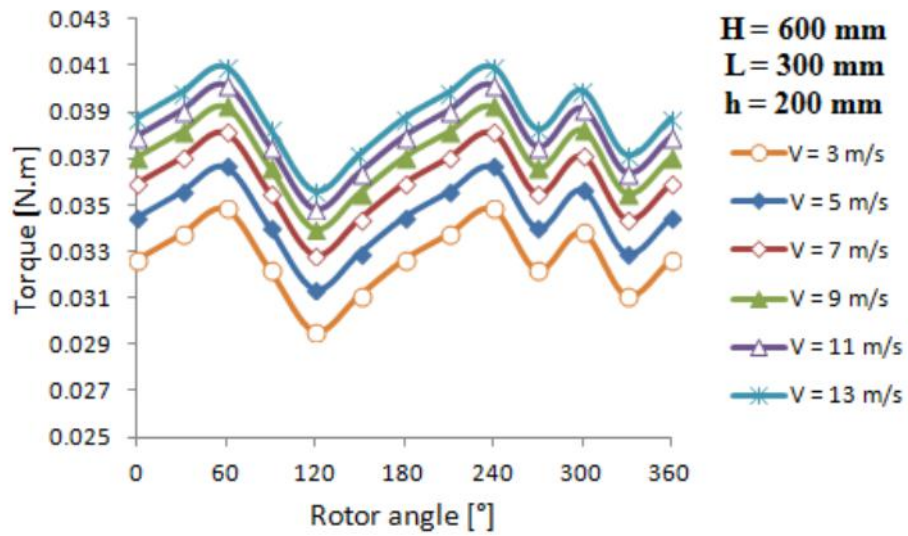


Figure 4.7: Static torque vs. angle of rotation for model 7

4.2 Mechanical Power of the Rotors of the first new configuration of Savonius rotors

Figures 4.8 to 4.14 illustrate the amount of mechanical power produced from a different new configuration of Savonius wind turbine rotors with varying wind speed, In this section, it shows the effect of the models on the mechanical power of the rotors. It is observed that the model has higher mechanical power than other models as shown in the figures. The conventional Savonius rotor (model 1) is produced the minimum mechanical power compared to other rotors. Furthermore, it is noticed that as the wind speed increases, the mechanical power of the rotors will increase. As mentioned previously, there are some factors can affect the static torque of the rotors like distance between rotor's blades, weight of the rotor and height of halves blades. Therefore, these factors have great influence on the angular velocity of the shaft of the rotor. As a result, mechanical power of the model 5, which was calculated by multiplying the static torque and angular velocity of the shaft, is higher than other models.

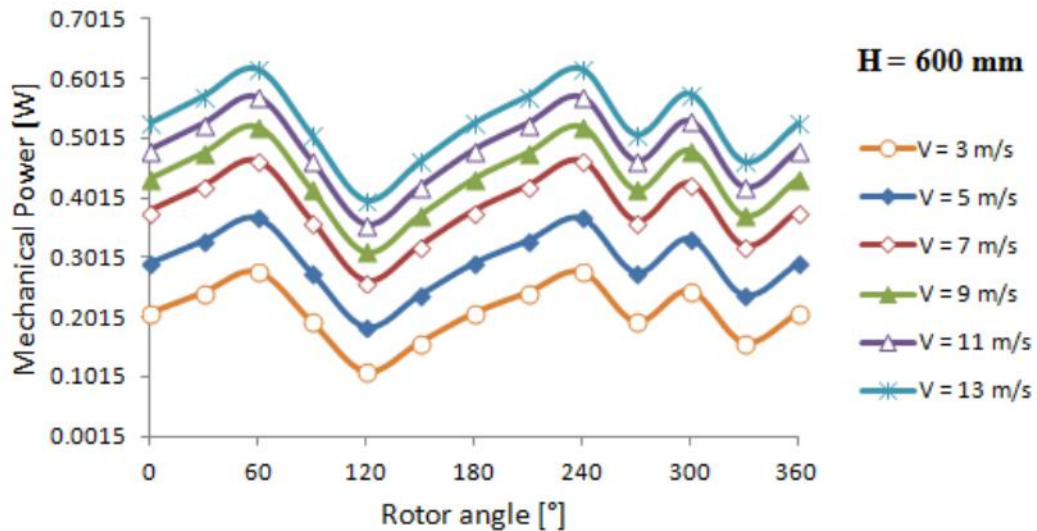


Figure 4.8: Mechanical power vs. angle of rotation for model 1

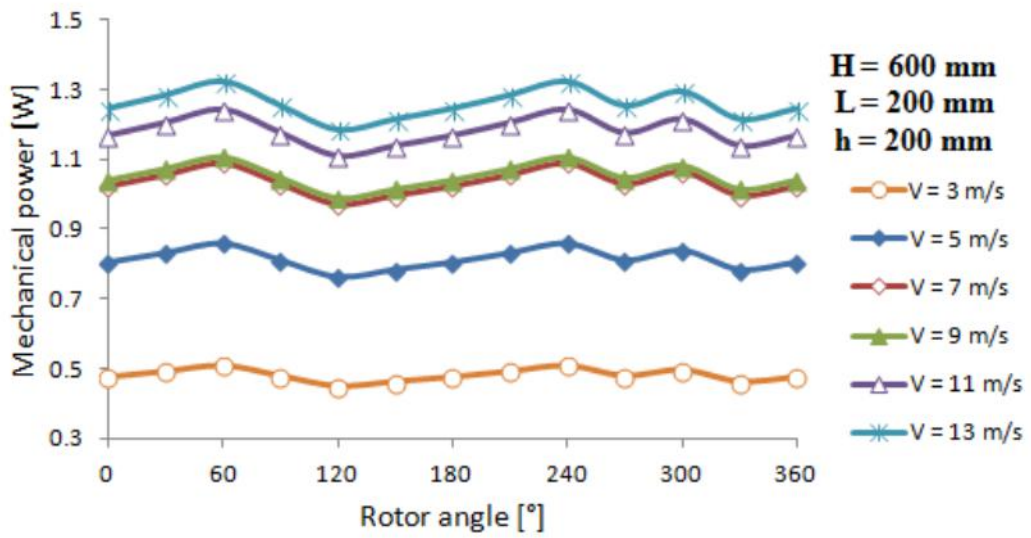


Figure 4.9: Mechanical power vs. angle of rotation for model 2

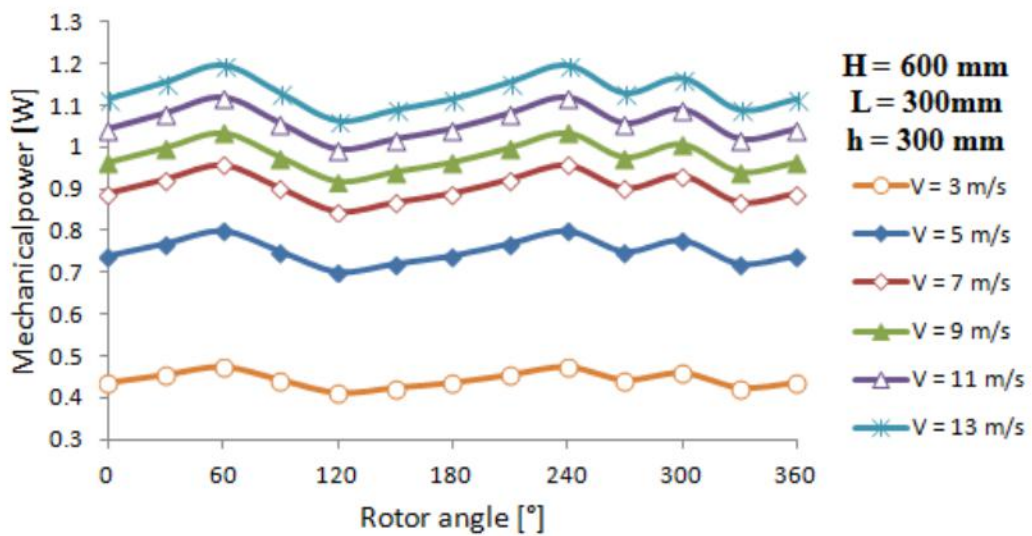


Figure 4.10: Mechanical power vs. angle of rotation for model 3

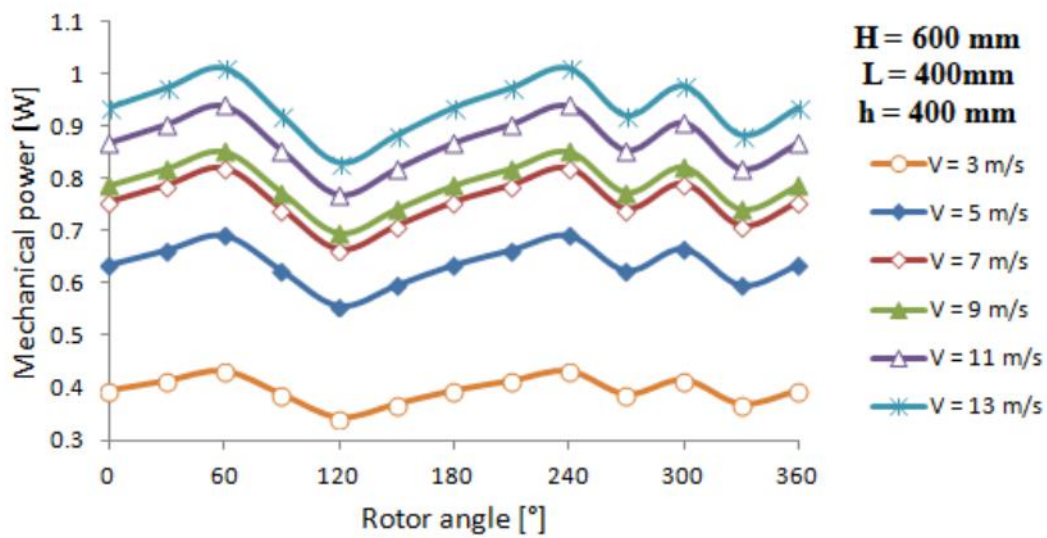


Figure 4.11: Mechanical power vs. angle of rotation for model 4

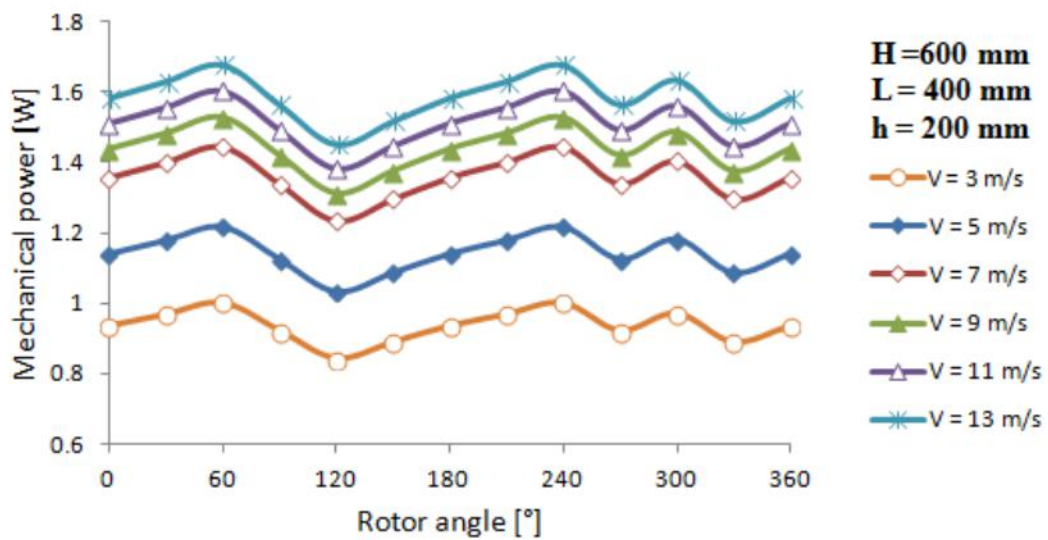


Figure 4.12: Mechanical power vs. angle of rotation for model 5

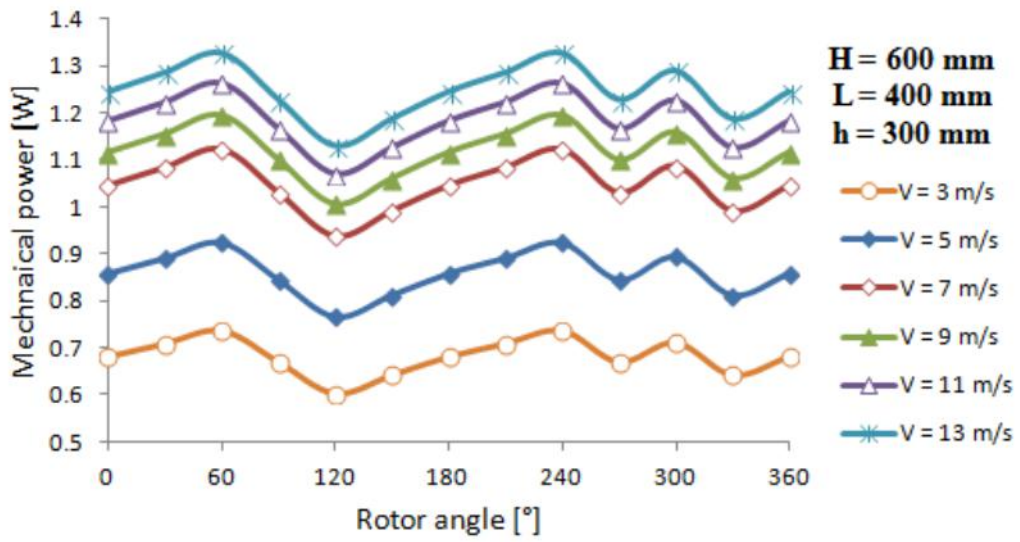


Figure 4.13: Mechanical power vs. angle of rotation for model 6

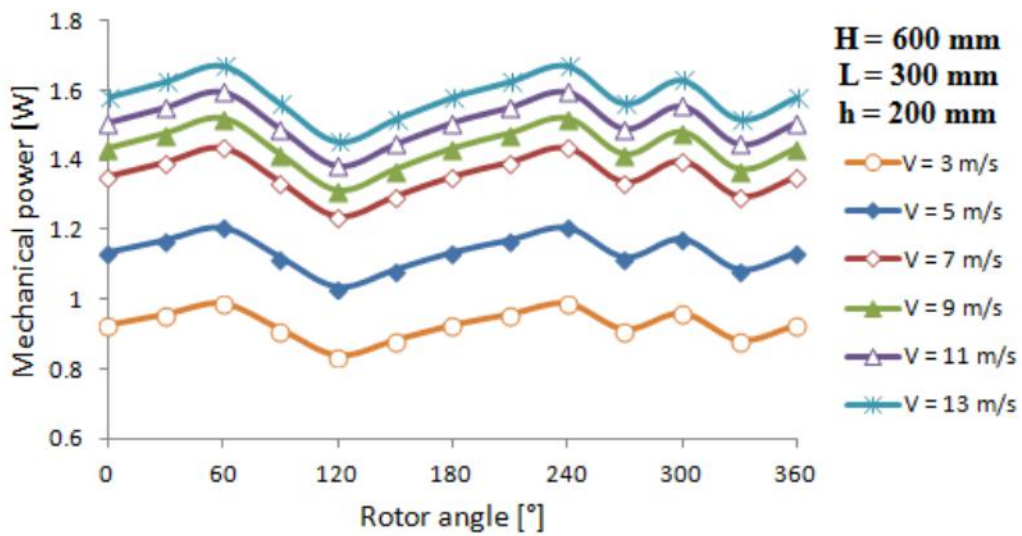


Figure 4.14: Mechanical power vs. angle of rotation for model 7

4.3 Effect of models on Static torque of the first new configuration of Savonius rotors

In this section, comparative study was carried out for seven new designs of Savonius wind rotors at various wind speeds (Figures 4.15 to 4.20). Figures 4.15 to 4.20 show the static torque of seven rotors as function of rotor angles (0° to 360° in steps of 30°). It observed that the static torque of all rotors increases when the wind speed increase. From these figures, it noticed that, the conventional Savonius rotor has minimum static torque compared to new designs of the rotors. Additionally, Model 7 has higher static torque than other models and the static torque for model 2 and 6 is almost equal as shown in Figures 4.15 to 4.20. This may be due to the net drag force affected on rotor in model 7 is higher than those for model 1 to model 6.

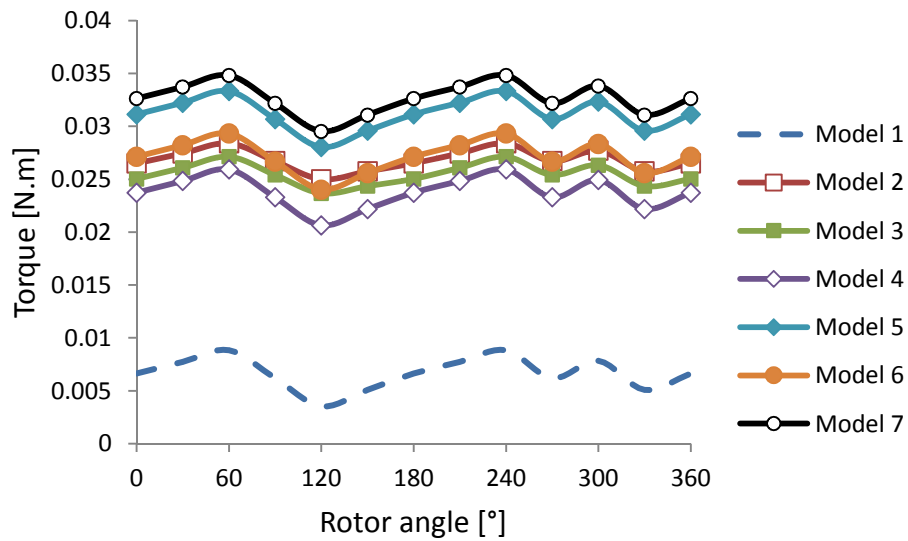


Figure 4.15: Static torque vs. rotor angle of first new configuration of rotors at 3 m/s

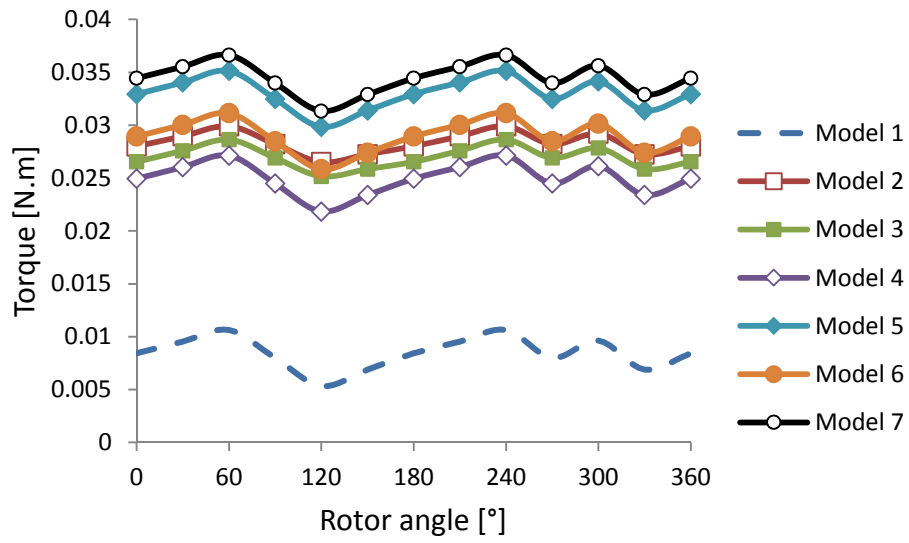


Figure 4.16: Static torque vs. rotor angle of first new configuration of rotors at 5 m/s

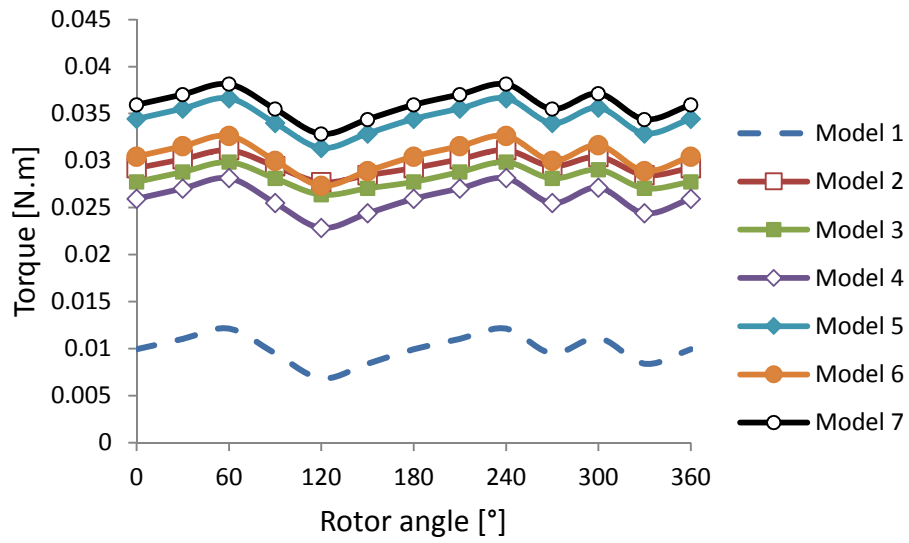


Figure 4.17: Static torque vs. rotor angle of first new configuration of rotors at 7 m/s

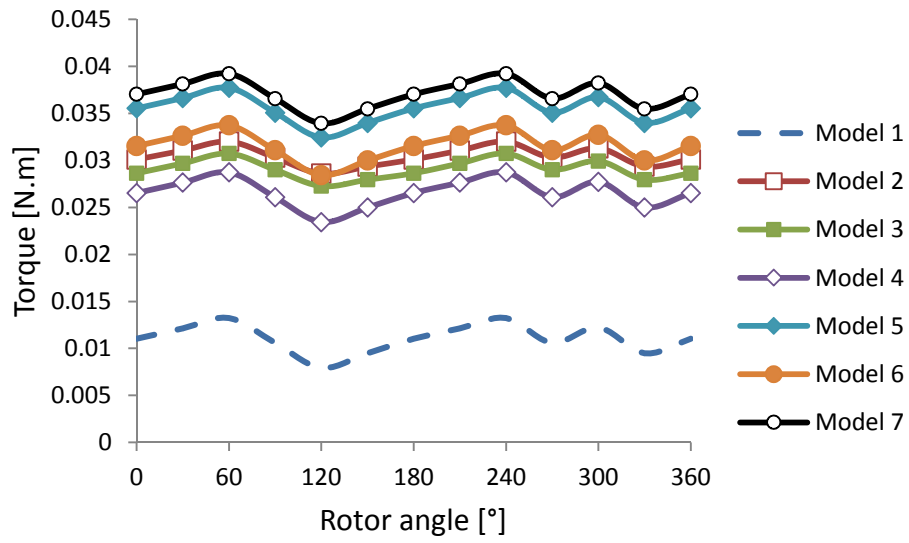


Figure 4.18: Static torque vs. rotor angle of first new configuration of rotors at 9 m/s

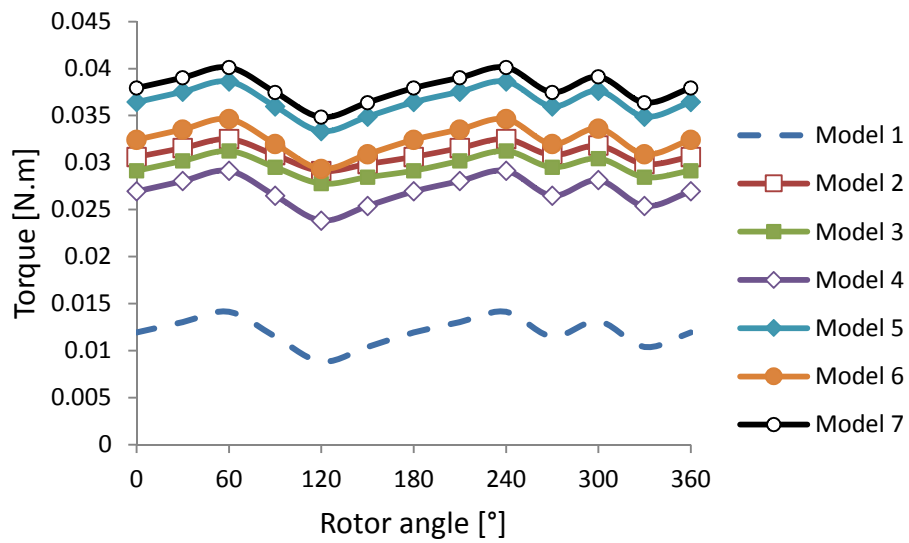


Figure 4.19: Static torque vs. rotor angle of first new configuration of rotors at 11 m/s

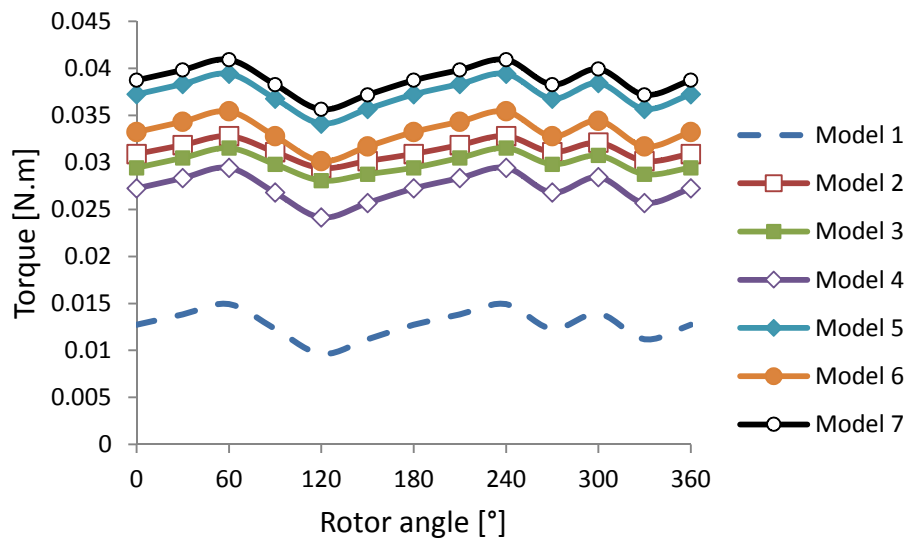


Figure 4.20: Static torque vs. rotor angle of first new configuration of rotors at 13 m/s

4.4 Effect of models on Mechanical Power of the first new configuration of Savonius rotors

The mechanical power of each model and combined wind speed effect of seven models variation with the change in rotor positions is shown in Figure 4.21 to 4.26. The plot is displayed at 30° interval from 0° to 360°. Compared to the conventional Savonius wind rotor with new seven designs of conventional Savonius rotors, the new developed rotor designs seem to able to gain some improvements in terms of mechanical power of the rotors. From the figures, it can be seen that the mechanical power of model 5 is higher than other models. Also, it can be observed that at high speed above 7 m/s, the mechanical power for both model 7 and 5 are almost equal. Wind turbine model with high variation between the height of halves blades (Model 5) or less weight of the rotor (Model 7) has more drag force (more torque) at any position when the wind rotor is in rotational position. Therefore, model 5 and 7 will deliver higher mechanical power of the turbine.

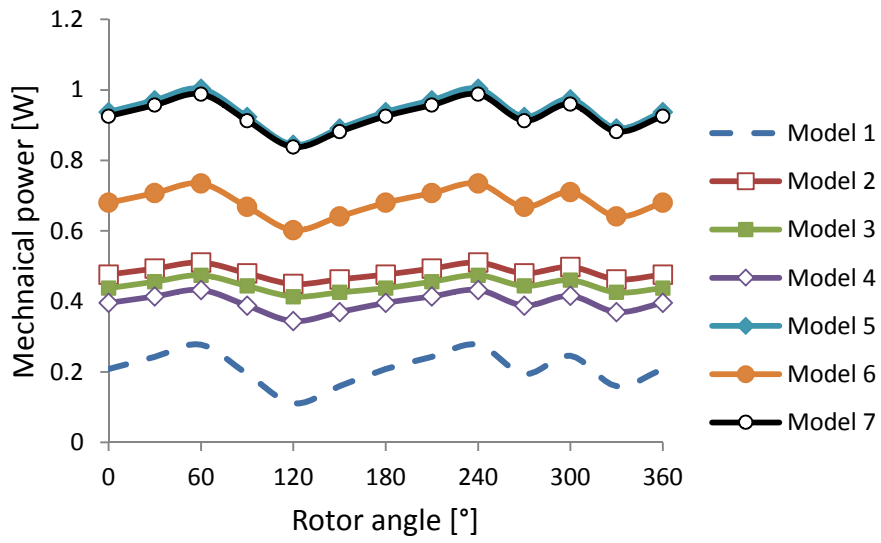


Figure 4.21: Mechanical power vs. rotor angle of first new configuration of rotors at 3 m/s

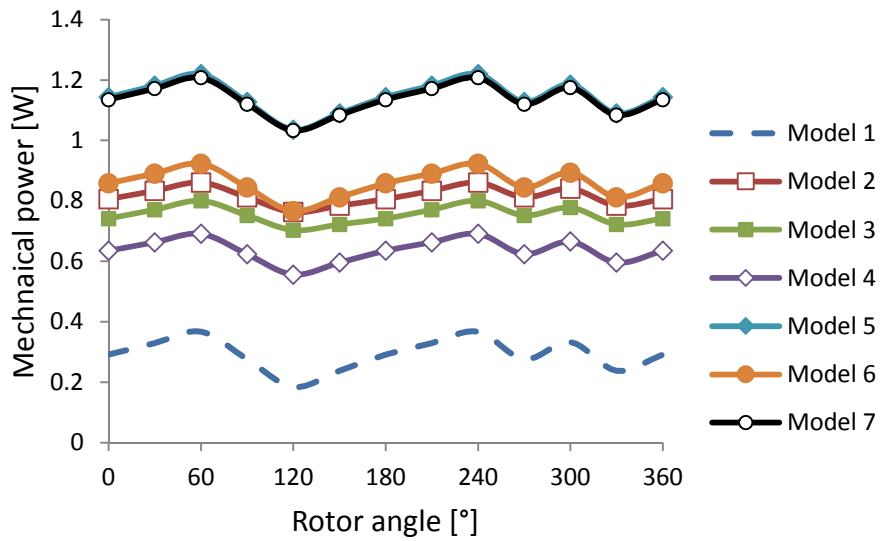


Figure 4.22: Mechanical power vs. rotor angle of first new configuration of rotors at 5 m/s

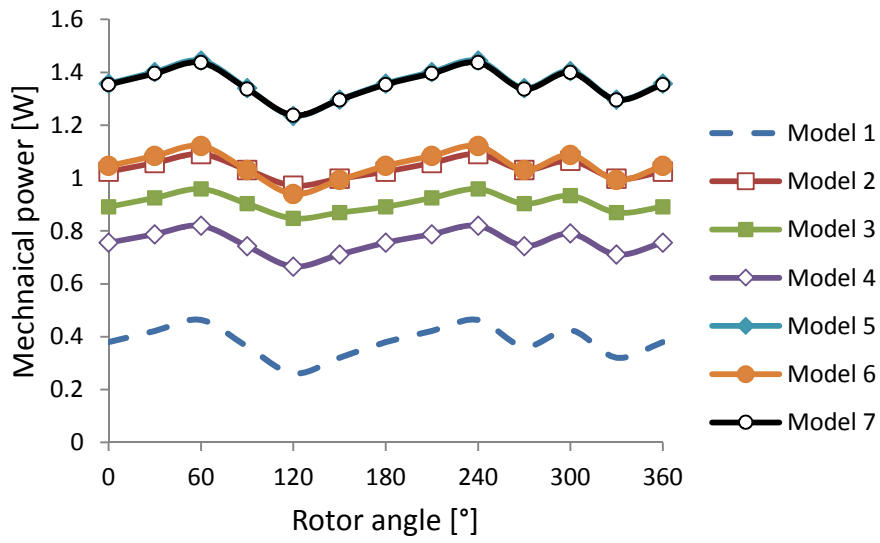


Figure 4.23: Mechanical power vs. rotor angle of first new configuration of rotors at 7m/s

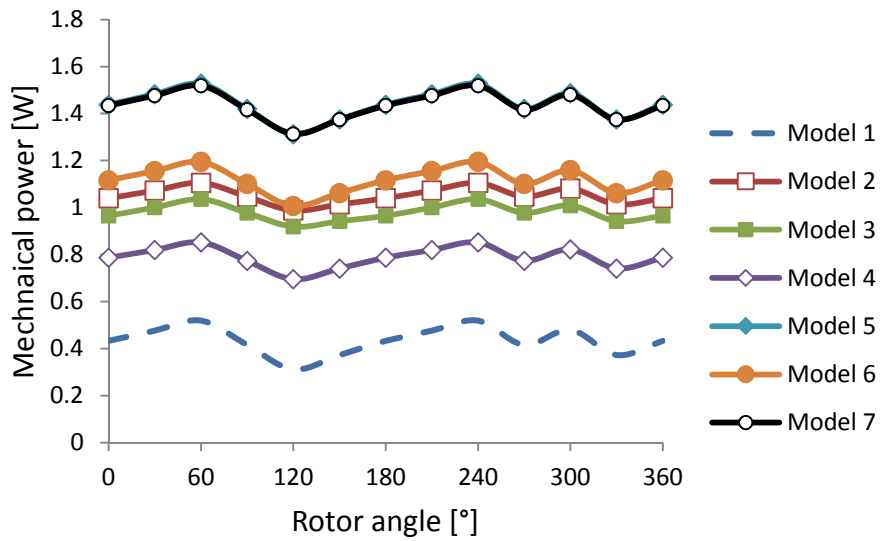


Figure 4.24: Mechanical power vs. rotor angle of first new configuration of rotors at 9 m/s

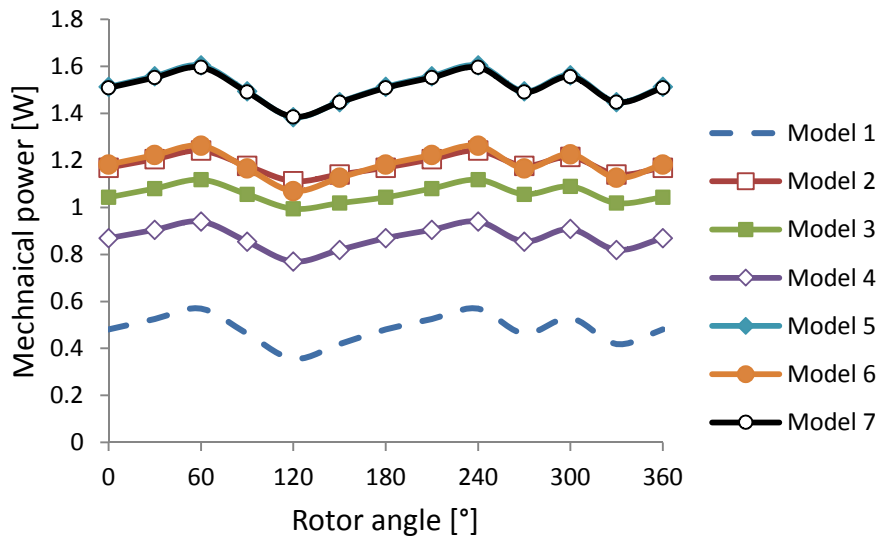


Figure 4.25: Mechanical power vs. rotor angle of first new configuration of rotors at 11 m/s

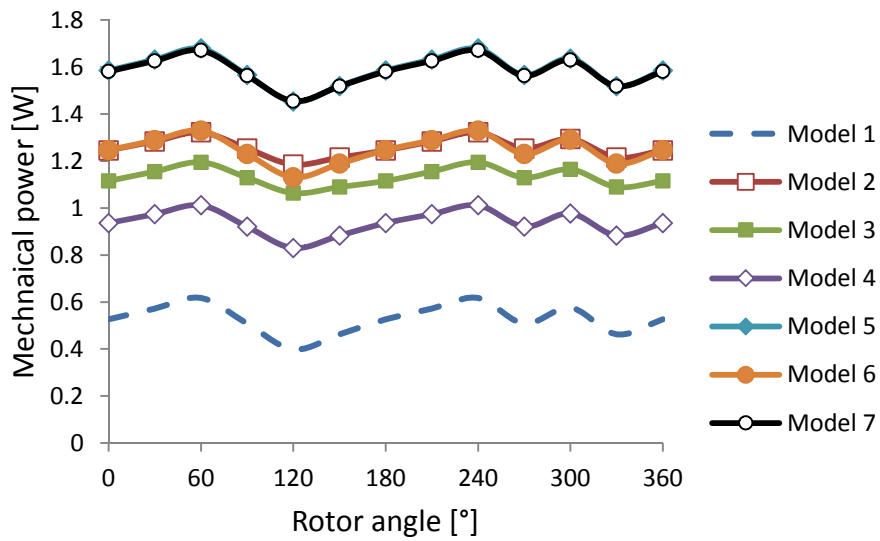


Figure 4.26: Mechanical power vs. rotor angle of first new configuration of rotors at 13 m/s

4.5 Effect of Wind Speed on Average Static Torque and Mechanical Power of the first new configuration of Savonius rotors

The average static torque (T_{average}) or mechanical power (MP_{average}), are calculated by dividing the sum of all values of static torque or mechanical power at a different rotor angle by a number of the values. It is given by the formula

$$T_{\text{average}} = \frac{\sum_{i=1}^n T_i}{n} \quad (4.1)$$

$$MP_{\text{average}} = \frac{\sum_{i=1}^n MP_i}{n} \quad (4.2)$$

Figures 4.27 and 4.28 illustrate the amount of average static torque and mechanical power produced from the seven models of Savonius wind turbine rotor with different at different wind speed, respectively. Additionally, the comparison between the average static torque and average mechanical power of the models are shown in these figures and Table 4.2. It can notice that the average static torque and mechanical power is rapidly increasing with the increase in wind speed. Moreover, conventional Savonius wind rotor (Model 1) has a lower average static torque and mechanical power compared to other models. From these Figures, it is clear that as the wind speed increase the average static torque or mechanical power of the new configuration of Savonius rotors will increase linearly.

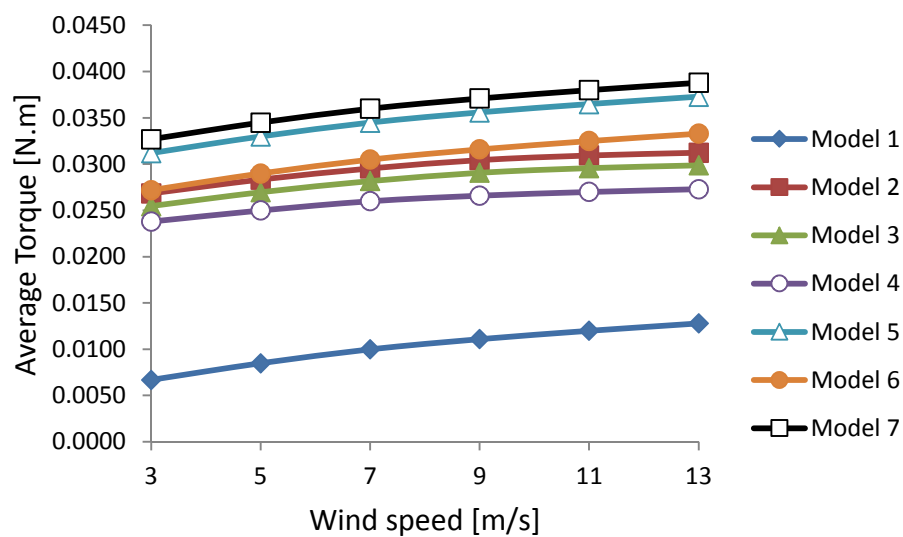


Figure 4.27: Average static torque vs. wind speed of first new configuration of rotors

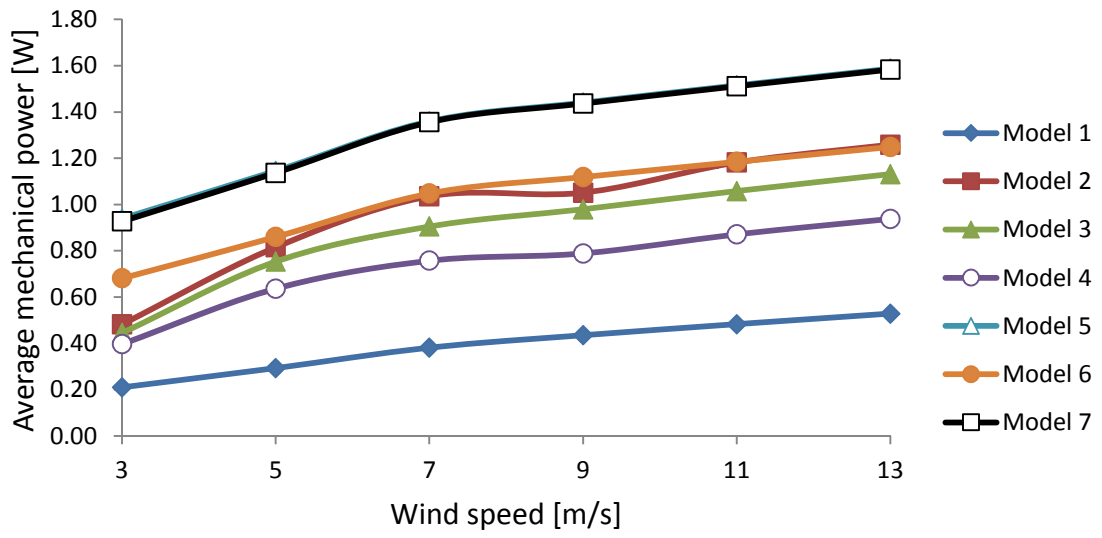


Figure 4.28: Average mechanical power vs. wind speed of first new configuration of rotors

Table 4.2: Comparatives average static torque and average mechanical power of the first new configuration of rotors

Model 1						
Wind speed [m/s]	3	5	7	9	11	13
RPM	300	330	365	375	385	395
Average Torque [N.m]	0.00668	0.008487	0.009987	0.011087	0.011987	0.01278
Average mechanical power [W]	0.20997	0.293147	0.381544	0.435172	0.483043	0.52865
Model 2						
Wind speed [m/s]	3	5	7	9	11	13
RPM	172	275	335	330	365	385
Average Torque [N.m]	0.02683	0.02833	0.02953	0.03043	0.03093	0.03123
Average mechanical power [W]	0.48209	0.81545	1.03545	1.05108	1.18166	1.25850
Model 3						
Wind speed [m/s]	3	5	7	9	11	13
RPM	167	267	307	322	342	362
Average Torque [N.m]	0.02546	0.026964	0.028164	0.029064	0.029564	0.02986
Average mechanical power [W]	0.44509	0.753539	0.904988	0.979538	1.058277	1.13153
Model 4						
Wind speed [m/s]	3	5	7	9	11	13
RPM	156	240	275	280	305	325
Average Torque [N.m]	0.02378	0.024987	0.025987	0.026587	0.026987	0.02728
Average mechanical power [W]	0.39669	0.636396	0.757064	0.788458	0.870936	0.93773
Model 5						
wind speed [m/s]	3	5	7	9	11	13
RPM	288	332	377	387	397	407
Average Torque [N.m]	0.03118	0.032987	0.034487	0.035587	0.036487	0.03728
Average mechanical power [W]	0.93901	1.145132	1.359638	1.440253	1.514867	1.58710
Model 6						
Wind speed [m/s]	3	5	7	9	11	13
RPM	239	283	328	338	348	358
Average Torque [N.m]	0.02719	0.02899	0.03049	0.03159	0.03249	0.03329
Average mechanical power [W]	0.68104	0.85963	1.04771	1.11857	1.18445	1.24845
Model 7						
Wind speed [m/s]	3	5	7	9	11	13
RPM	271	315	360	370	380	390
Average Torque [N.m]	0.03268	0.034487	0.035987	0.037087	0.037987	0.03878
Average mechanical power [W]	0.92716	1.137042	1.355997	1.436263	1.510877	1.58329

4.6 Effect of RPM on Average Static Torque and Mechanical Power of the Rotors of the first new configuration of Savonius rotors

The effect of rotational speed (RPM) of the average static torque and mechanical power of the rotors are shown in Figures 4.29 and 4.30, respectively. From the results obtained, the Model 7 has higher RPM than other models. In general, the average static torque or average mechanical power increases when RPM of the rotors increase.

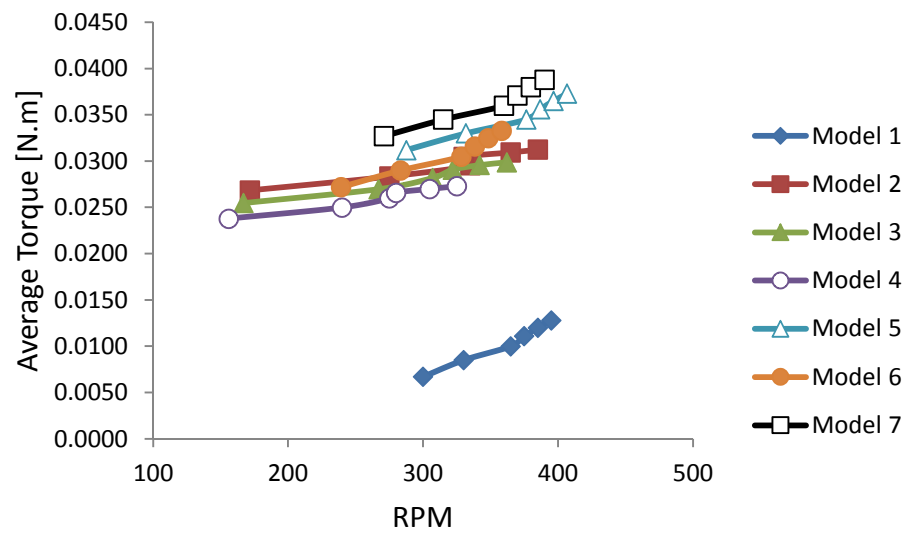


Figure 4.29: Average static torque vs. RPM of first new configuration of rotors

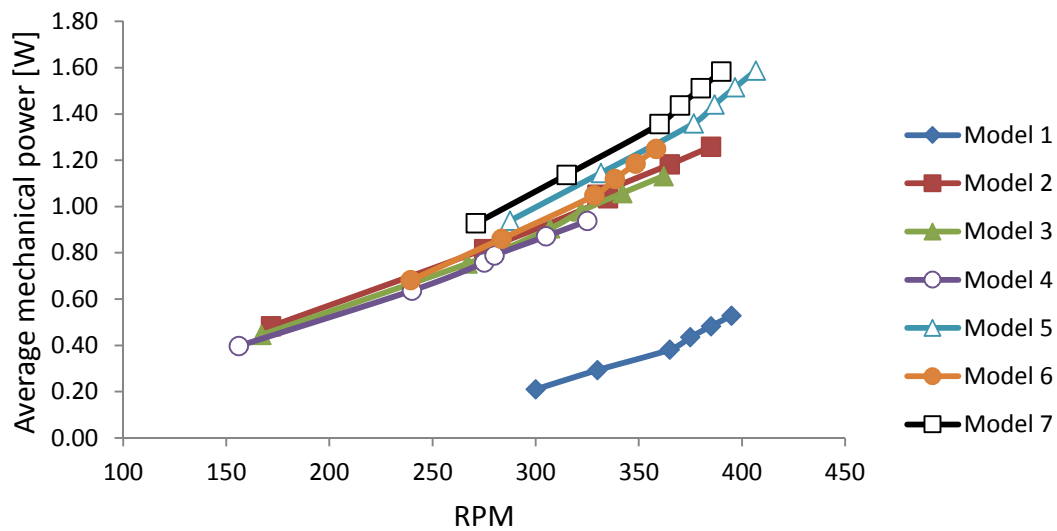


Figure 4.30: Average mechanical power vs. RPM of first new configuration of rotors

4.7 Static Torque of the Rotors of the second new configuration of Savonius rotors

The static torque of the second design of Savonius rotors varies of rotor position at different wind speed is shown in Figures 4.31 to 4.36. It is seen that as wind speed increases the static torque of rotors increases rapidly. Moreover, static torque of the new configuration of Savonius wind rotors starts to increase from (0° to 60°) to reach its highest value and then goes down to decrease from (60° to 120°) to reach the minimum value. And it is increased slightly from (120° to 180°), then rapidly increasing to get to the peak value (240°). The static torque of the rotors is getting the lowest value at 300° . Additionally, it is observed that static torque of all models is almost equal as shown in Figures 4.31 to 4.36. The results clearly showed that the torque output is almost equal as the intervals between the blades stack are same. As one might expected when the wind speed increases, the rotor torque output also increases.

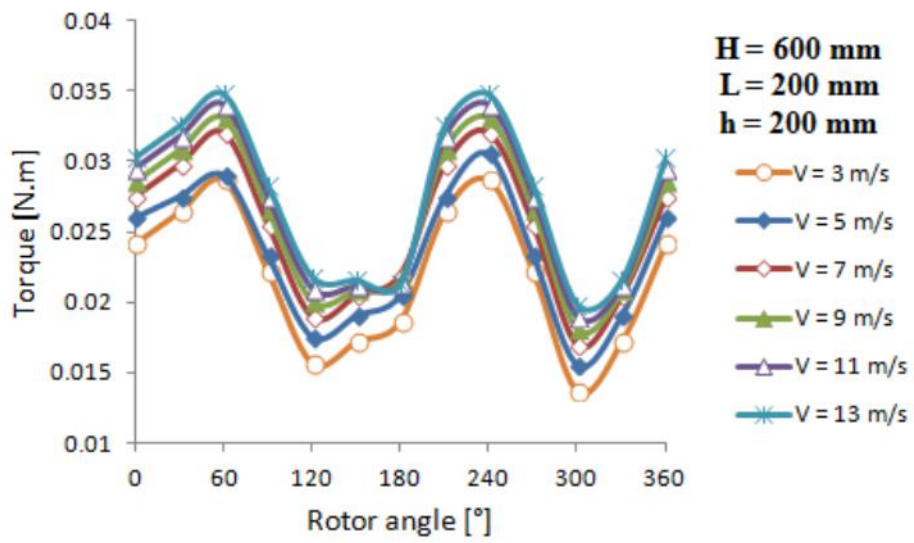


Figure 4.31: Static torque vs. angle of rotation for model 8

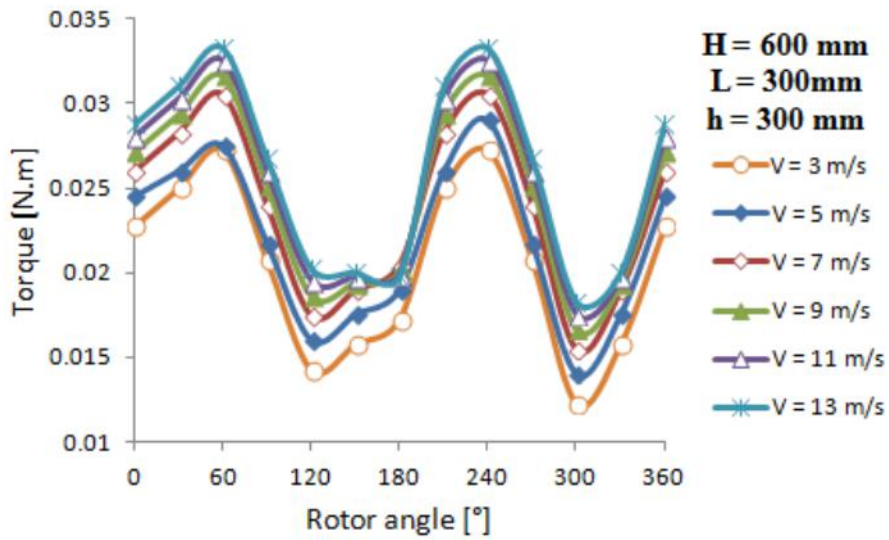


Figure 4.32: Static torque vs. angle of rotation for model 9

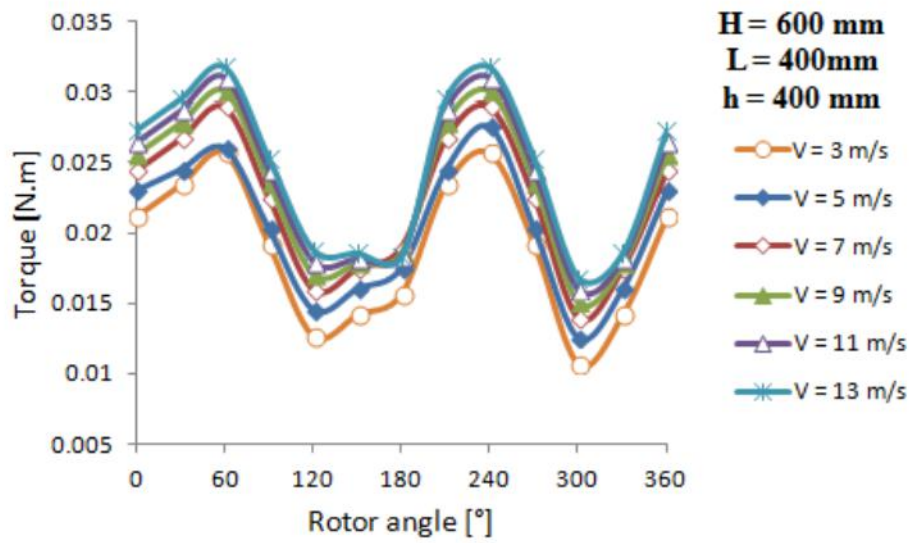


Figure 4.33: Static torque vs. angle of rotation for model 10

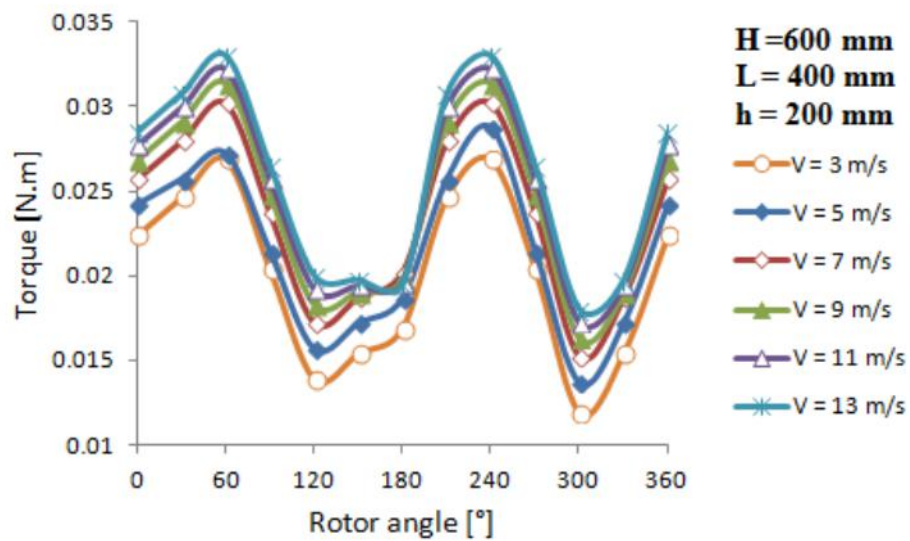


Figure 4.34: Static torque vs. angle of rotation for model 11

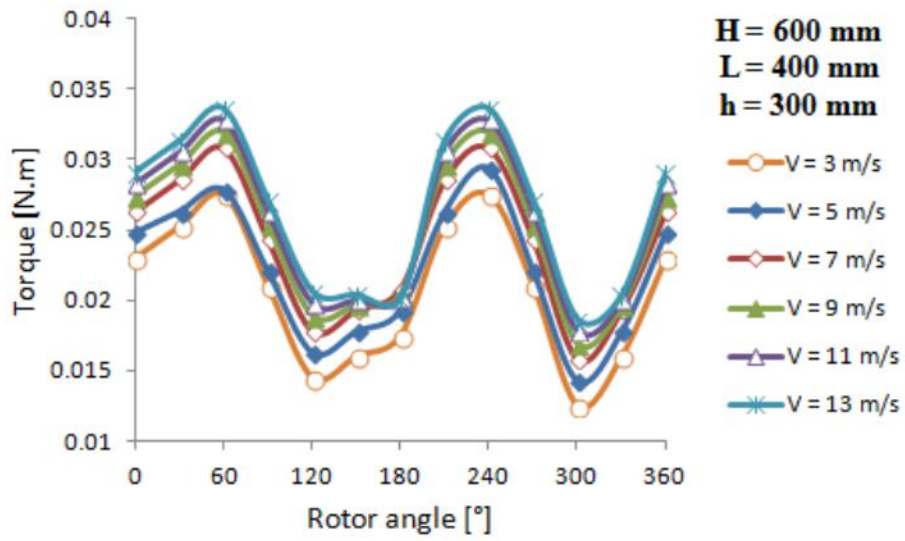


Figure 4.35: Static torque vs. angle of rotation for model 12

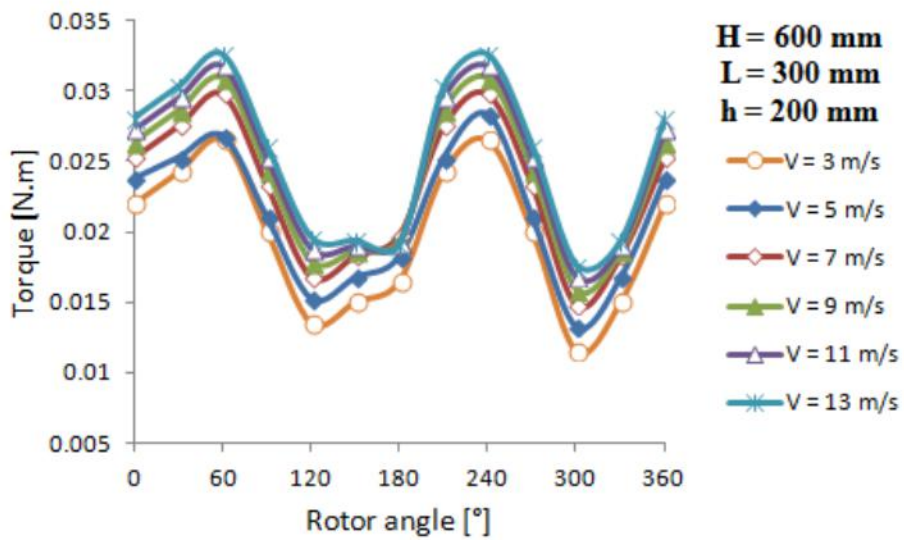


Figure 4.36: Static torque vs. angle of rotation for model 13

4.8 Mechanical power of the Rotors of the second new configuration of Savonius rotors

The mechanical power produced from different models (model 8, 9, 10, 11, 12, and 13) with varying wind speed and rotor positions are shown in Figures 4.37 to 4.42. It is observed that the model 8 has higher mechanical power than other models as shown in the figures. The conventional Savonius rotor (model 1) is produced the minimum mechanical power compared to other rotors. Furthermore, it is noticed that as the wind speed increases, the mechanical power of the rotors will increase. Similarity, weight of the rotor has great impact on the angular velocity of the shaft of the rotor. As a result, mechanical power of the model 8, which was calculated by multiplying the static torque and angular velocity of the shaft, is higher than other models.

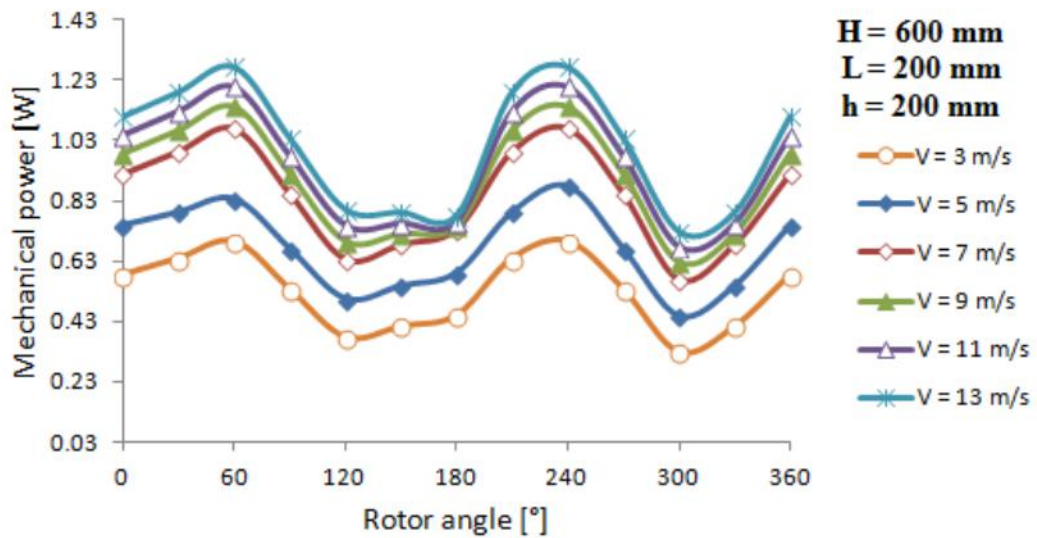


Figure 4.37: Mechanical power vs. angle of rotation for model 8

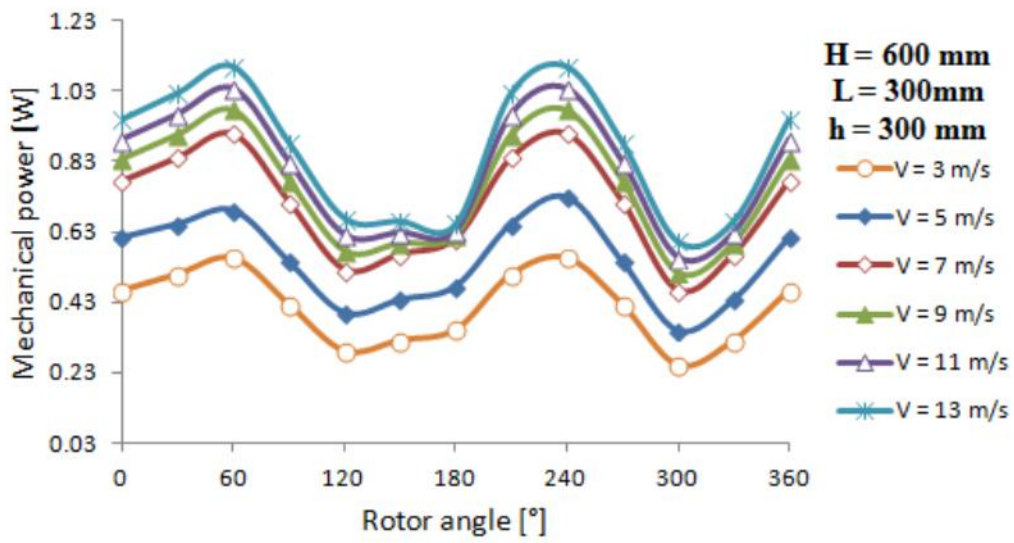


Figure 4.38: Mechanical power vs. angle of rotation for model 9

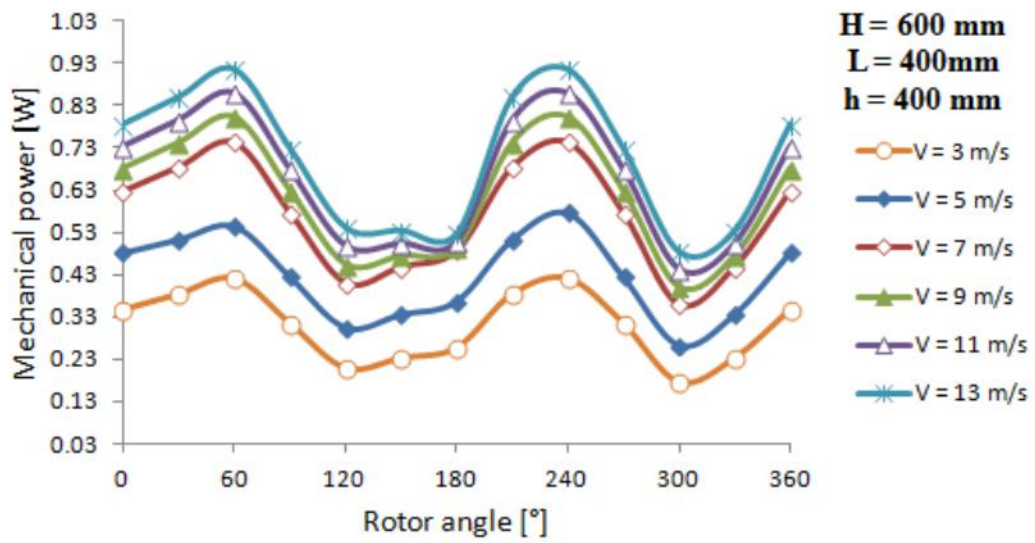


Figure 4.39: Mechanical power vs. angle of rotation for model 10

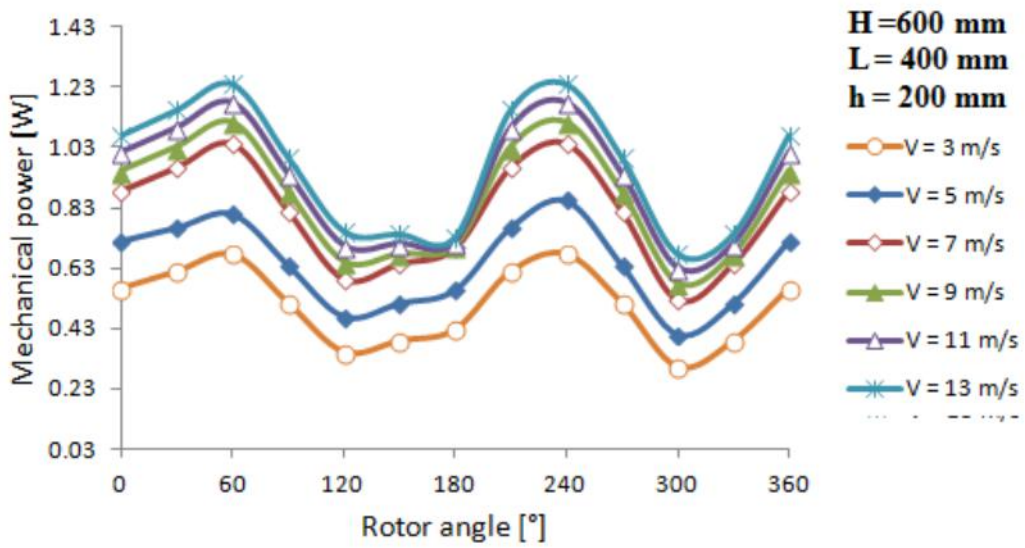


Figure 4.40: Mechanical power vs. angle of rotation for model 11

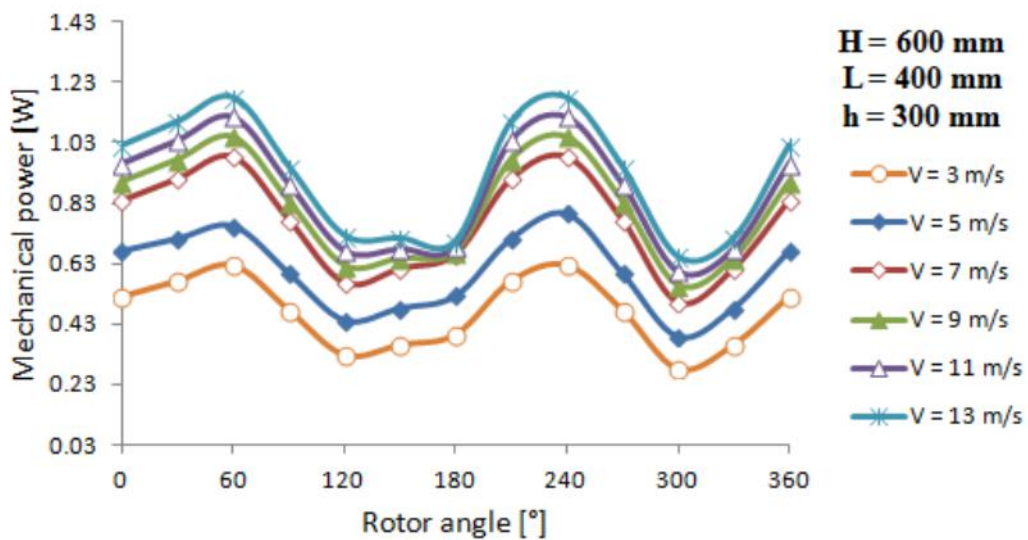


Figure 4.41: Mechanical power vs. angle of rotation for model 12

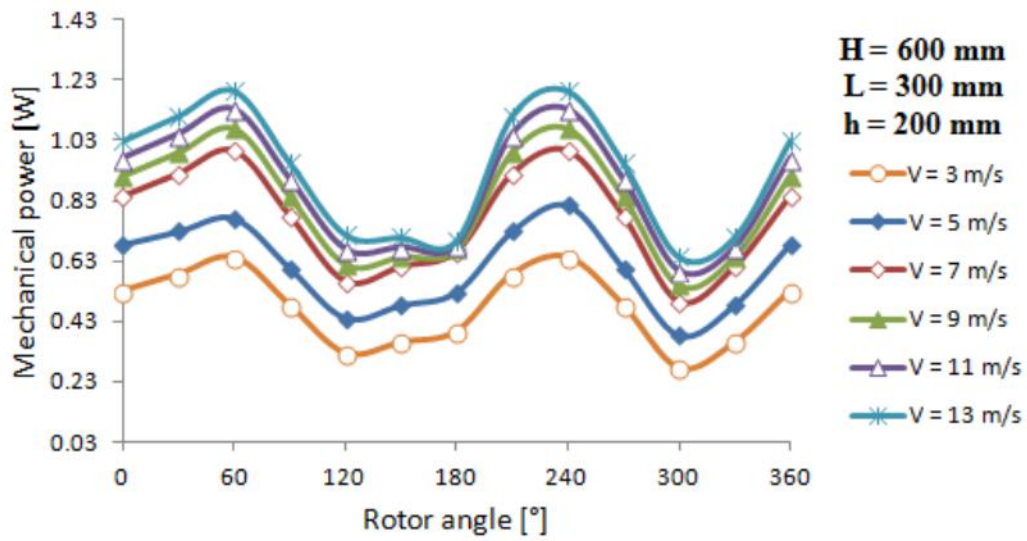


Figure 4.42: Mechanical power vs. angle of rotation for model 13

4.9 Effect of models on Static power of second new configuration of Savonius rotors

In this section, comparative study was carried out for six new designs of Savonius wind rotors (second configuration) at various wind speeds (Figures 4.43 to 4.48). The effect of rotor positions and wind speed on the static torque of the models are revealed in Figures 4.43-4.48. According to the comparative study, increase in wind speed leads to increase the static torque of the models. It is noticed that, model 8 has the highest static torque compared to model 1, 9, 10, 12 and 13.

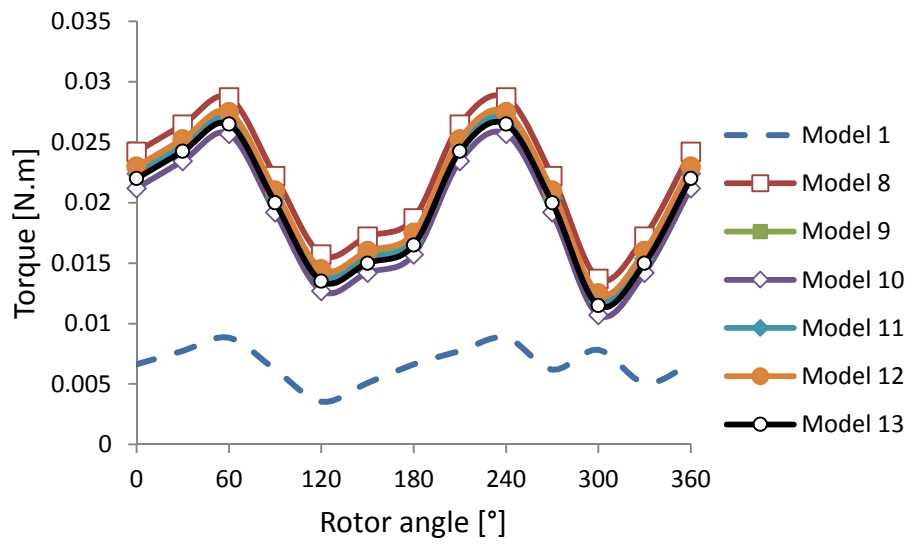


Figure 4.43: Static torque vs. rotor angle of second configuration of rotors at 3 m/s

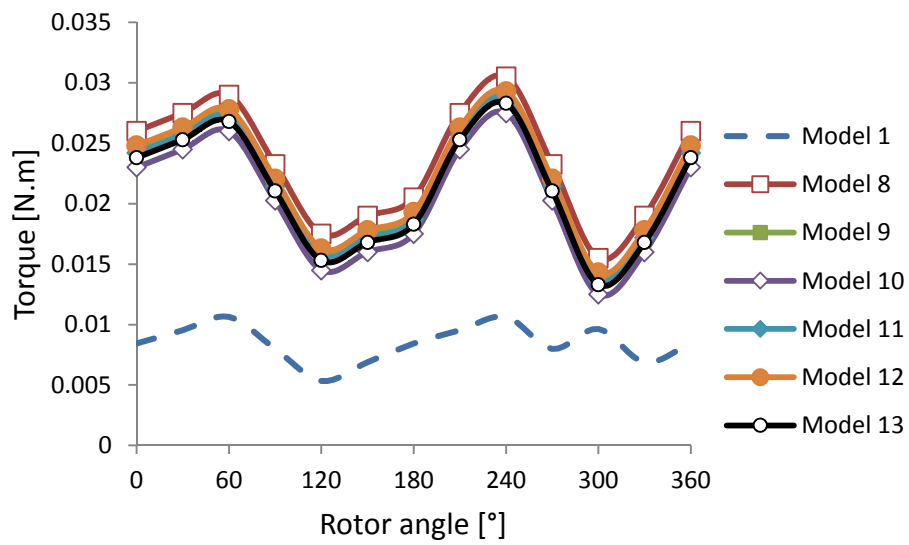


Figure 4.44: Static torque vs. rotor angle of second configuration of rotors at 5 m/s

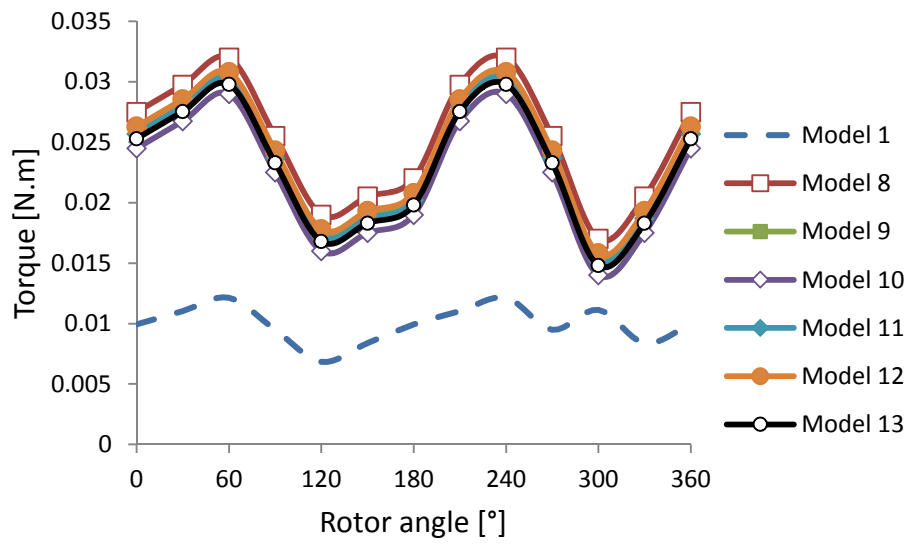


Figure 4.45: Static torque vs. rotor angle of second configuration of rotors at 7 m/s

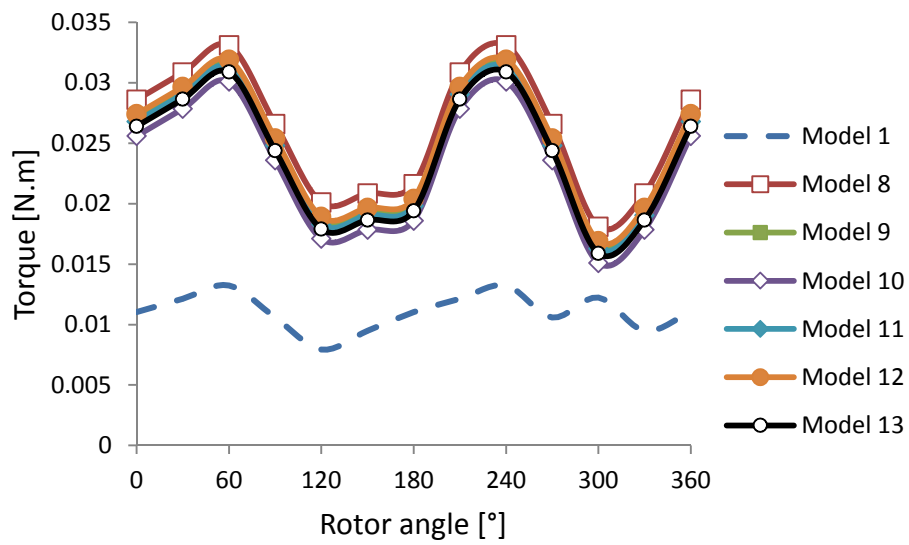


Figure 4.46: Static torque vs. rotor angle of second configuration of rotors at 9 m/s

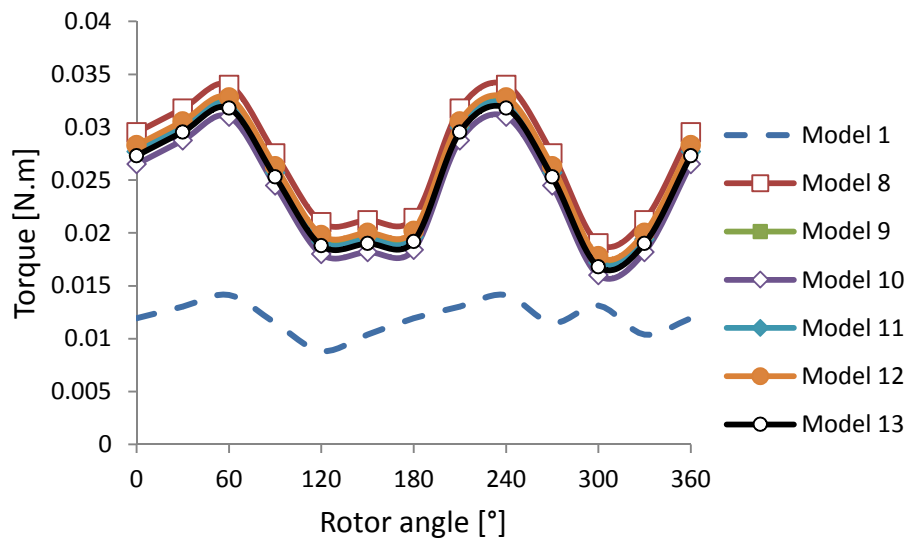


Figure 4.47: Static torque vs. rotor angle of second configuration of rotors at 11 m/s

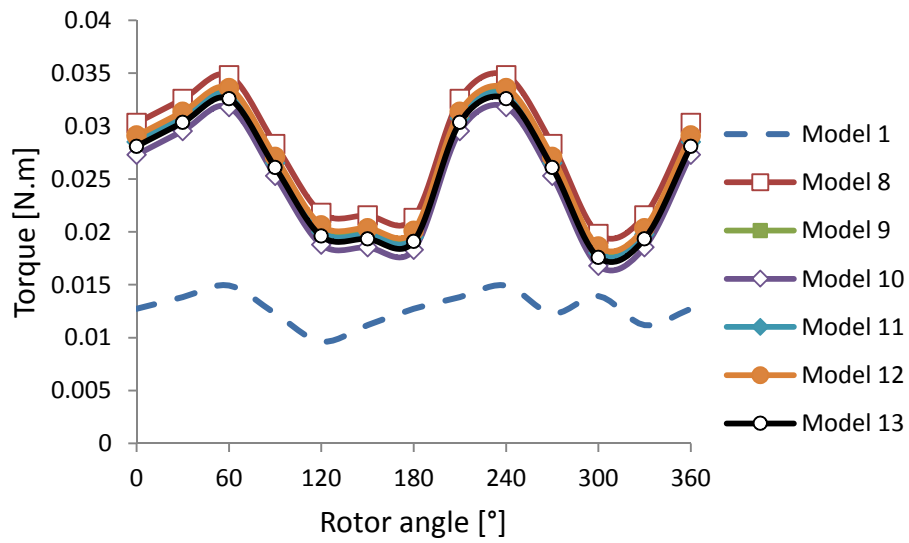


Figure 4.48: Static torque vs. rotor angle of second configuration of rotors at 13 m/s

4.10 Effect of models on Mechanical power of second new configuration of Savonius rotors

The effect of wind speed and blade height of halves blades on the The mechanical power of second configuration of Savonius rotors are shown in Figure 4.49 to 4.54. The plot is displayed at 30° interval from 0° to 360°. Compared to the conventional Savonius wind rotor with new designs of conventional Savonius rotors, the new developed rotor designs seem too able to gain some improvements in terms of mechanical power of the rotors. From the figures, it can be seen that the mechanical power of model 8 is higher than other models. Also, it can be observed that the mechanical power for both model 8 and 11 are almost equal.

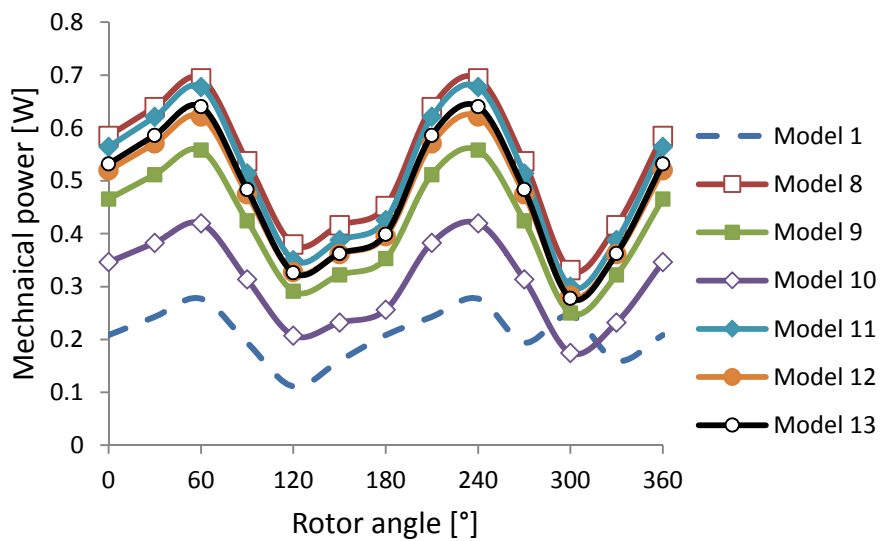


Figure 4.49: Mechanical power vs. rotor angle of second configuration of rotors at 3 m/s

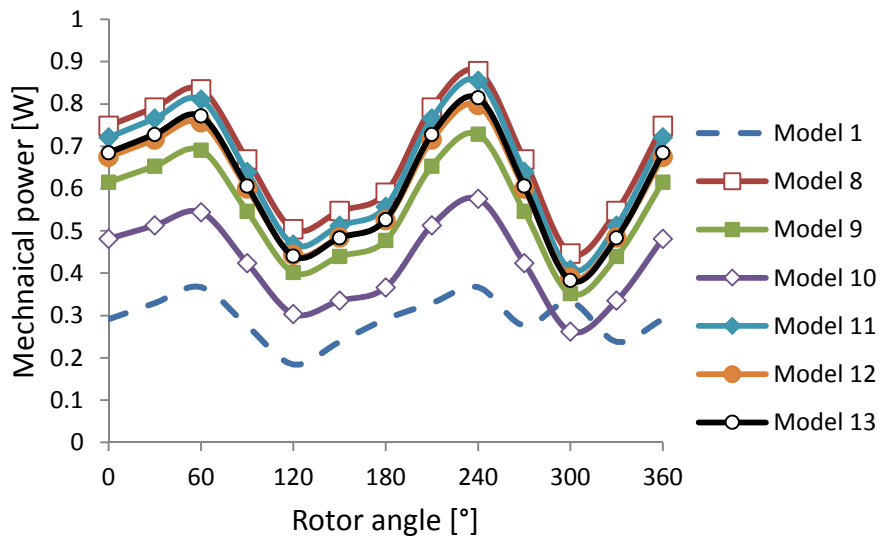


Figure 4.50: Mechanical power vs. rotor angle of second configuration of rotors at 5 m/s

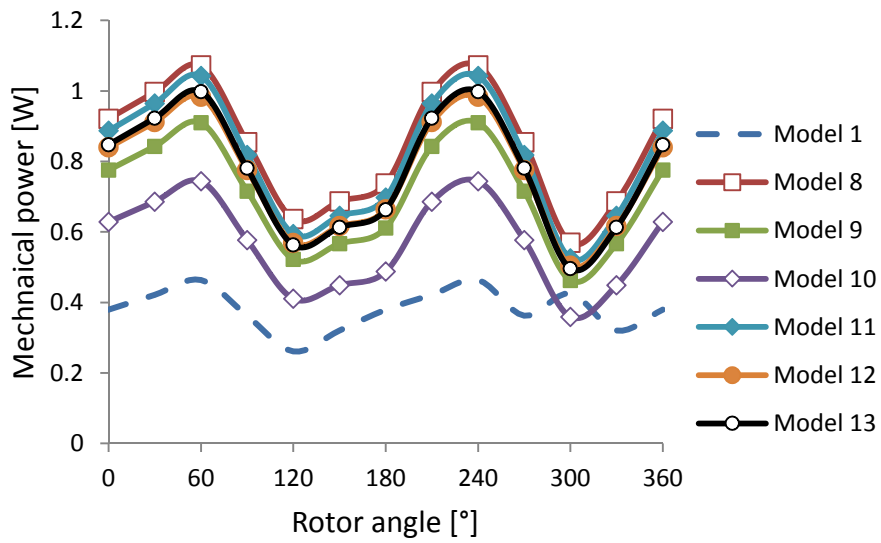


Figure 4.51: Mechanical power vs. rotor angle of second configuration of rotors at 7 m/s

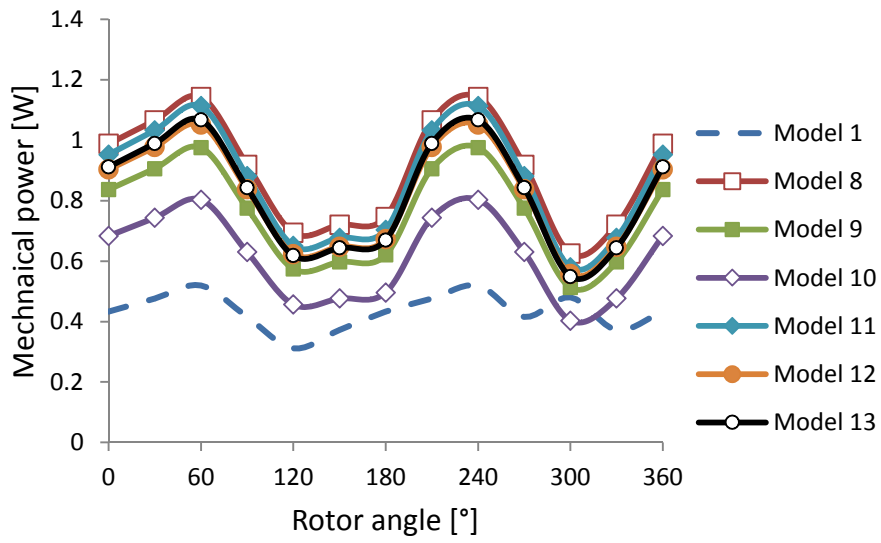


Figure 4.52: Mechanical power vs. rotor angle of second configuration of rotors at 9 m/s

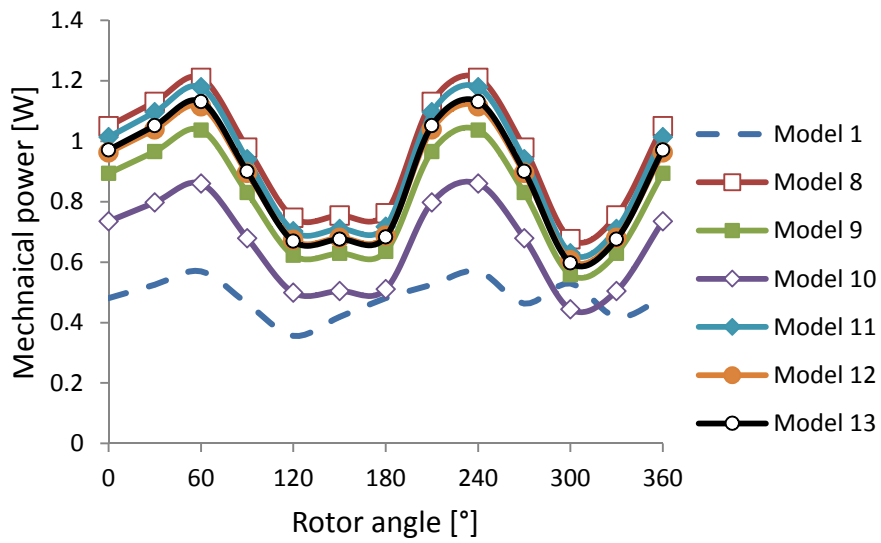


Figure 4.53: Mechanical power vs. rotor angle of second configuration of rotors at 11 m/s

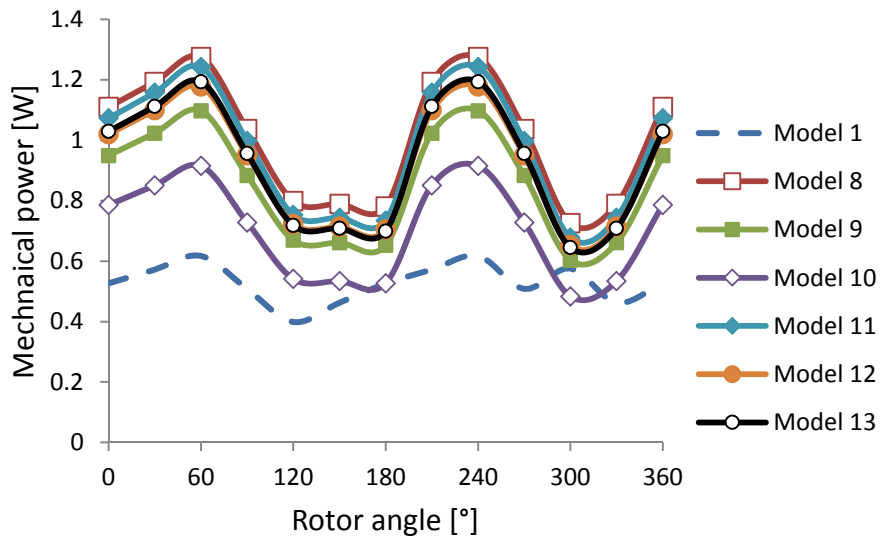


Figure 4.54: Mechanical power vs. rotor angle of second configuration of rotors at 13 m/s

4.11 Effect of wind speed Average Static Torque and Mechanical Power of the Rotors of the second new configuration of Savonius rotors

Figures 4.55 and 4.56 demonstrate the amount of average static torque and mechanical power produced from the rotors with different at different wind speed, respectively. Additionally, the comparison between the average static torque and average mechanical power of the models are shown in these figures and Table 4.3. It can notice that the average static torque and mechanical power is rapidly increasing with the increase in wind speed. From these Figures and table, it is clear that as the wind speed increase the average static torque or mechanical power of the new configuration of Savonius rotors will increase non-linearly.

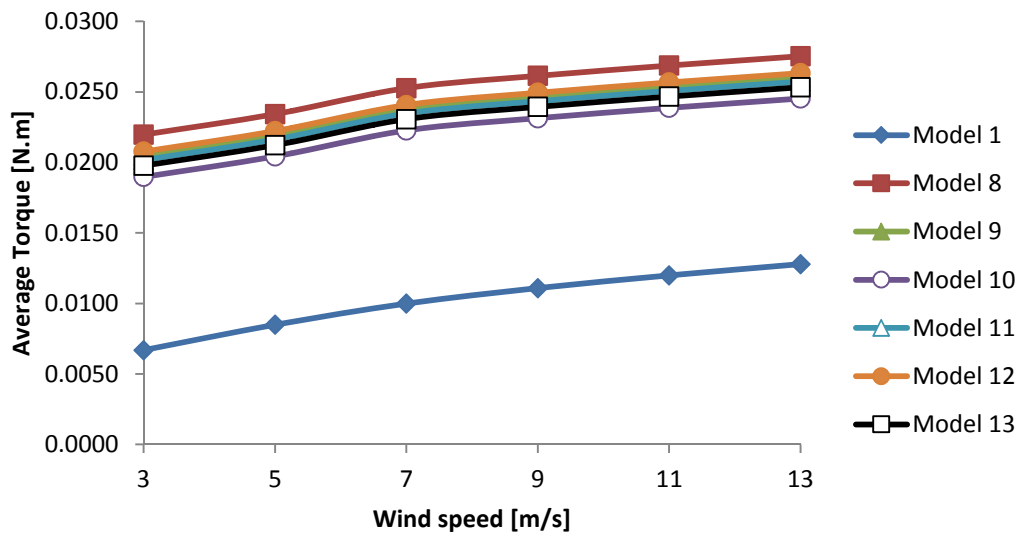


Figure 4.55: Average static torque vs. wind speed of second new configuration of rotors

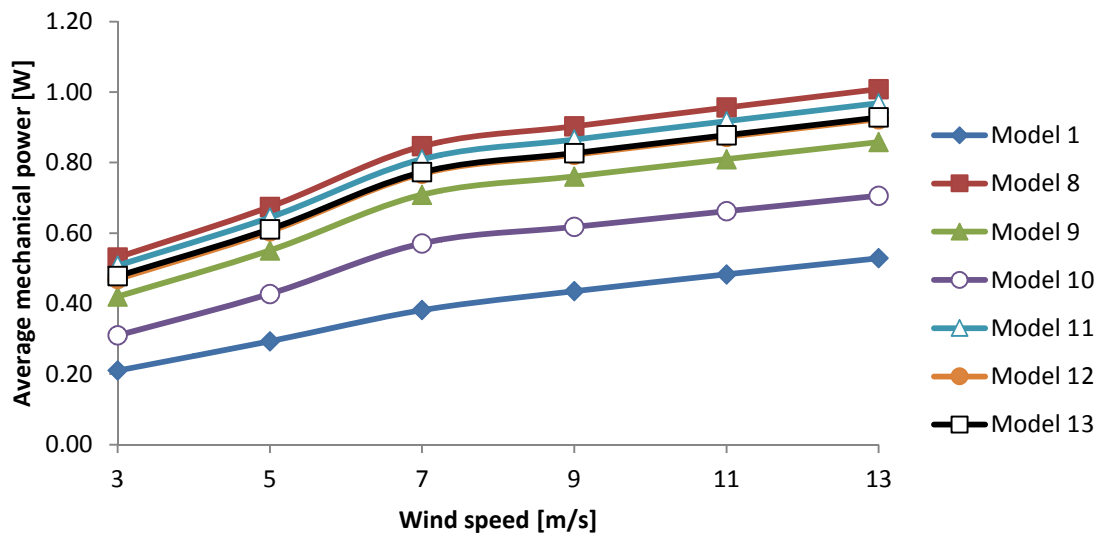


Figure 4.56: Average mechanical power vs. wind speed of second new configuration of rotors

Table 4.3: Comparatives average static torque and average mechanical power of the second new configuration of rotors

Model 1						
Wind speed [m/s]	3	5	7	9	11	13
RPM	300	330	365	375	385	395
Average Torque [N.m]	0.006687	0.008487	0.009987	0.011087	0.011987	0.012787
Average mechanical power [W]	0.209977	0.293147	0.381544	0.435172	0.483043	0.528665
Model 8						
Wind speed [m/s]	3	5	7	9	11	13
RPM	231	275	320	330	340	350
Average Torque [N.m]	0.02197	0.02342	0.02527	0.02614	0.02687	0.02753
Average mechanical power [W]	0.53117	0.67419	0.84635	0.90282	0.95619	1.00854
Model 9						
Wind speed [m/s]	3	5	7	9	11	13
RPM	196	240	285	295	305	315
Average Torque [N.m]	0.020469	0.021923	0.023769	0.024638	0.025369	0.026031
Average mechanical power [W]	0.419919	0.550708	0.709036	0.760754	0.809870	0.858234
Model 10						
Wind speed [m/s]	3	5	7	9	11	13
RPM	156	200	245	255	265	275
Average Torque [N.m]	0.018969	0.020423	0.022269	0.023138	0.023869	0.024531
Average mechanical power [W]	0.309730	0.427523	0.571057	0.617566	0.662053	0.706077
Model 11						
Wind speed [m/s]	3	5	7	9	11	13
RPM	241	285	330	340	350	360
Average Torque [N.m]	0.020169	0.021623	0.023469	0.024338	0.025069	0.025731
Average mechanical power [W]	0.508058	0.644262	0.809808	0.865276	0.917495	0.968638
Model 12						
Wind speed [m/s]	3	5	7	9	11	13
RPM	216	260	305	315	325	335
Average Torque [N.m]	0.02077	0.02222	0.02407	0.02494	0.02567	0.02633
Average mechanical power [W]	0.46955	0.60476	0.76837	0.82222	0.87318	0.92324
Model 13						
Wind speed [m/s]	3	5	7	9	11	13
RPM	231	275	320	330	340	350
Average Torque [N.m]	0.019769	0.021223	0.023069	0.023938	0.024669	0.025331
Average mechanical power [W]	0.477980	0.610871	0.772665	0.826834	0.877896	0.927951

4.12 Effect of RPM Average Static Torque and Mechanical Power of the Rotors of the second new configuration of Savonius rotors

The effect of RPM on the average static torque and mechanical power of the rotors are shown in Figures 4.57 and 4. 58, respectively. From the results obtained, the Model 8 has higher RPM than other models. In general, the average static torque or average mechanical power increases when RPM of the rotors increase.

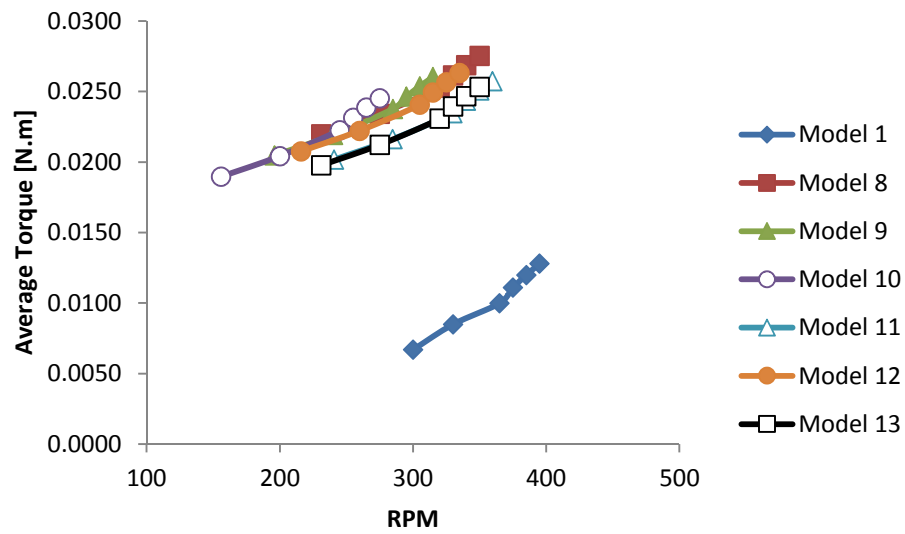


Figure 4.57: Average static torque vs. RPM of second new configuration of rotors

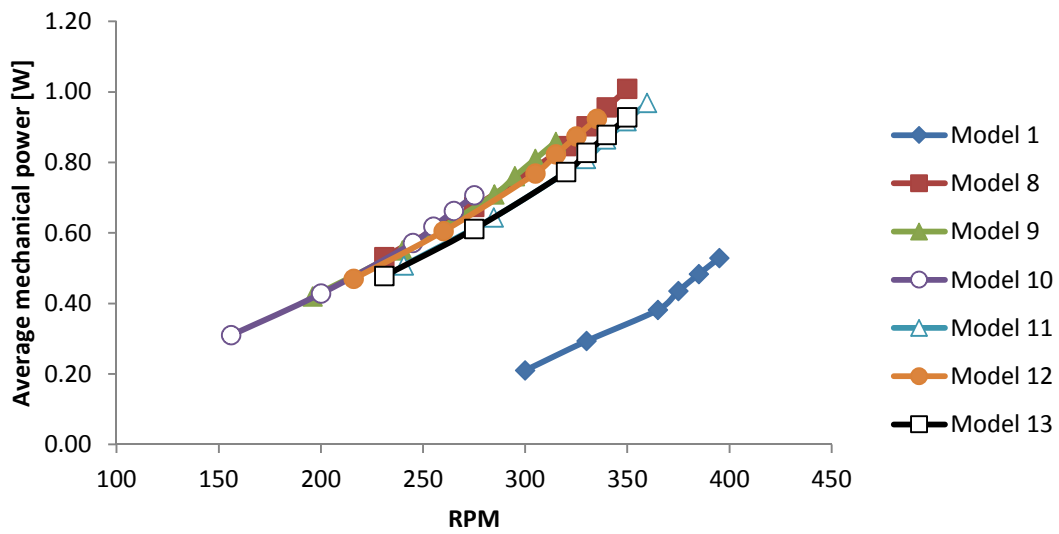


Figure 4.58: Average mechanical power vs. RPM of second new configuration of rotors

4.13 Comparison between first and second configuration of the rotors

In this section, the effect of the first and second configuration of Savonius wind rotors on the average static torque and mechanical power as a function of wind speed or RPM is shown in Figures 4.59 to 4.63. It is observed that the first configuration has higher static torque and mechanical power than the second configurations. Because for larger main blade distance or thickness, the fluid easily flows around the blades and as a result the torque output decreases. Comparing the both configuration with conventional Savonius rotor (model 1), both configurations have higher static torque and mechanical power than conventional Savonius rotor. Because the distance between the blades is greater the input wind flow easily back removed and a little momentum is built. Therefore, the torque output increases as the intervals between the blade stacks decrease.

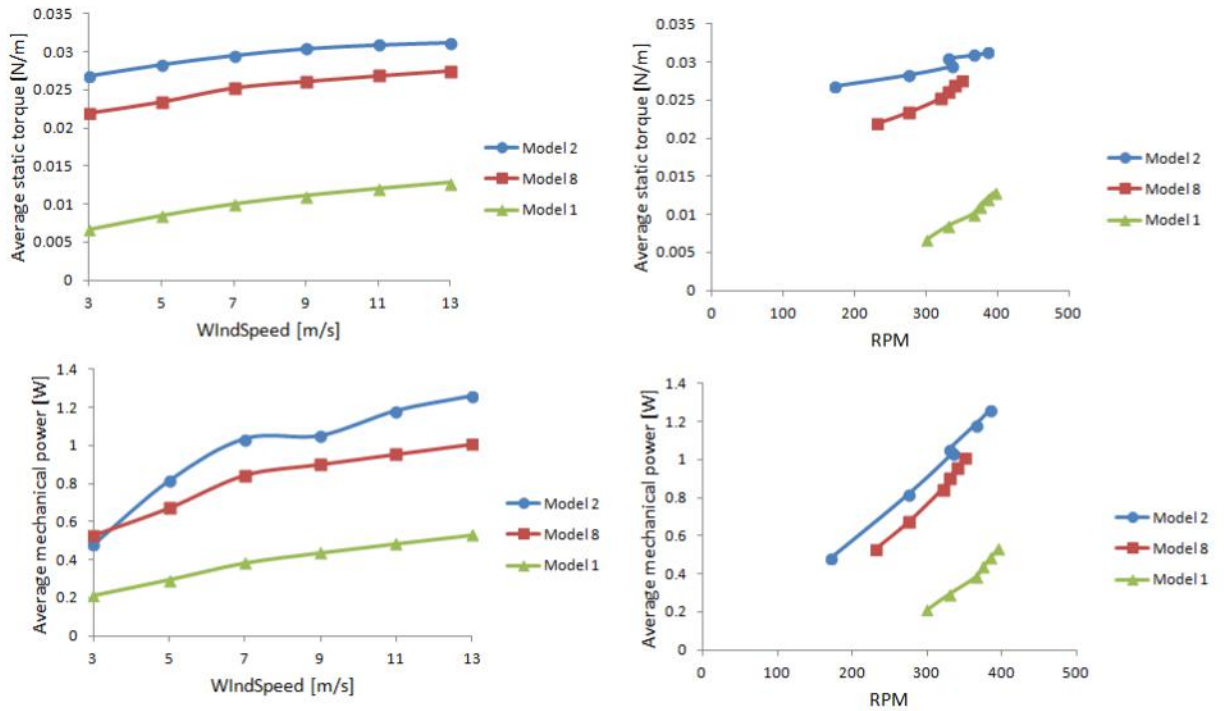


Figure 4.59: Comparison static torque and mechanical power of model 1, 2 and 8

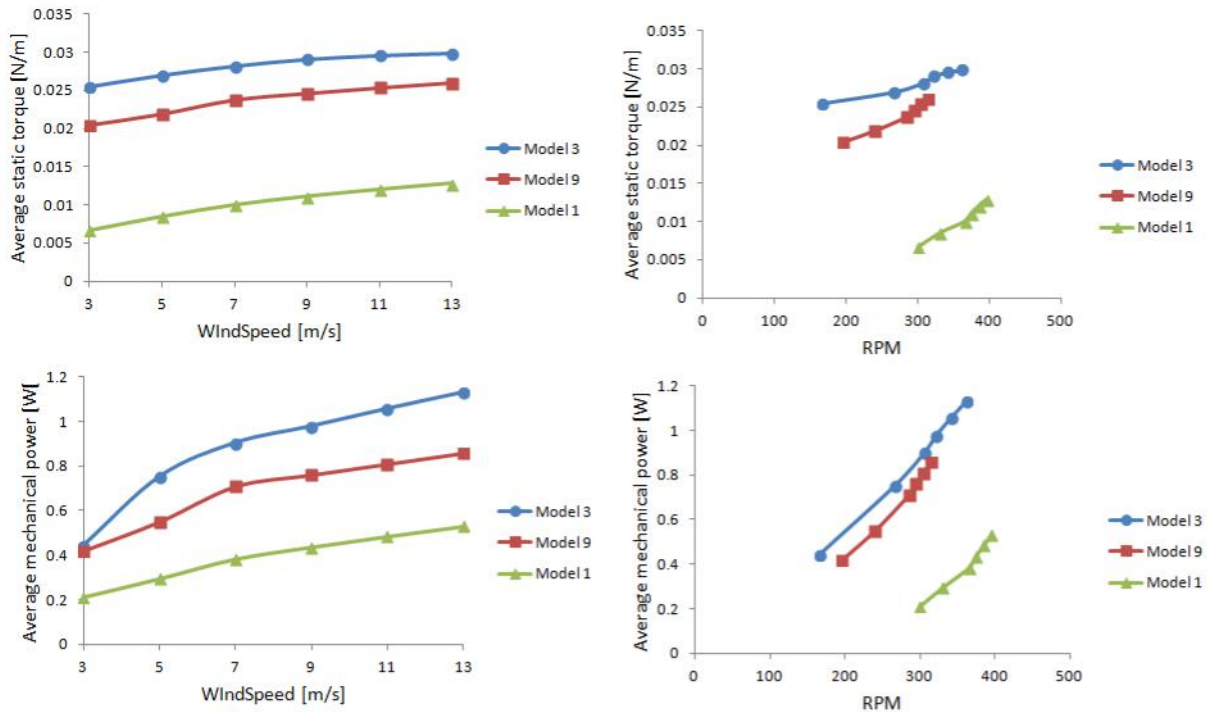


Figure 4.60: Comparison static torque and mechanical power of model 1, 3 and 9

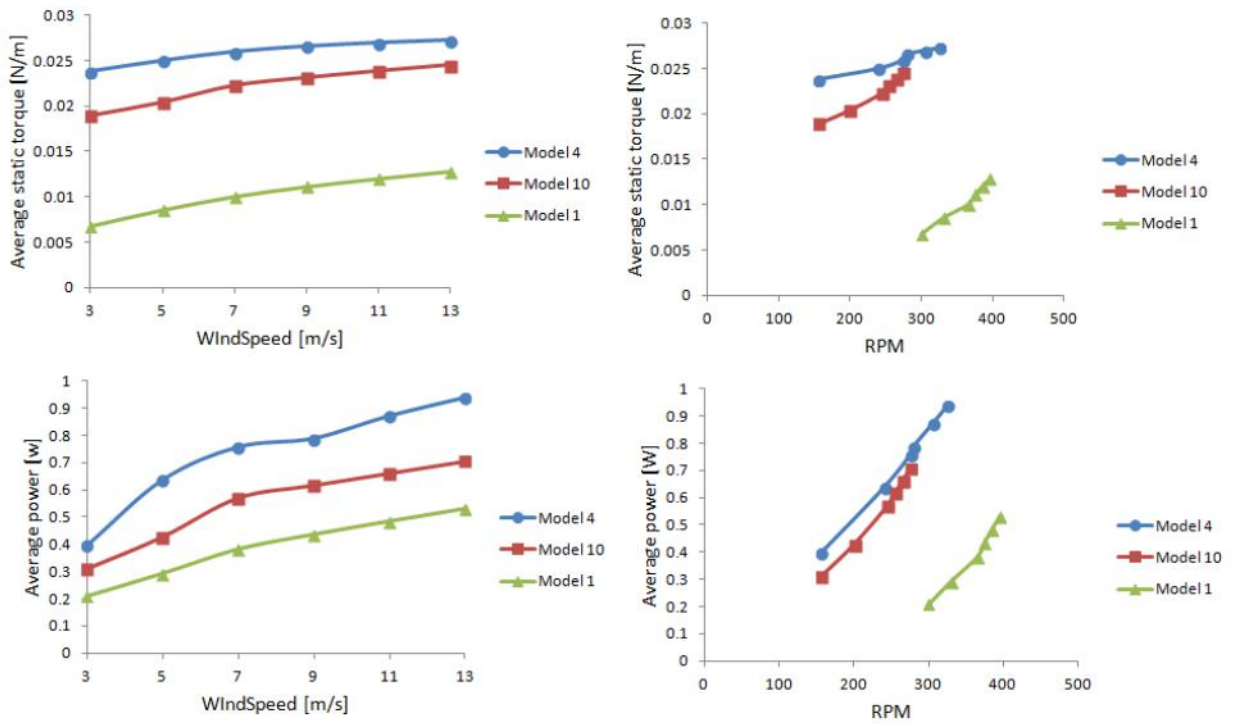


Figure 4.61: Comparison static torque and mechanical power of model 1, 4 and 10

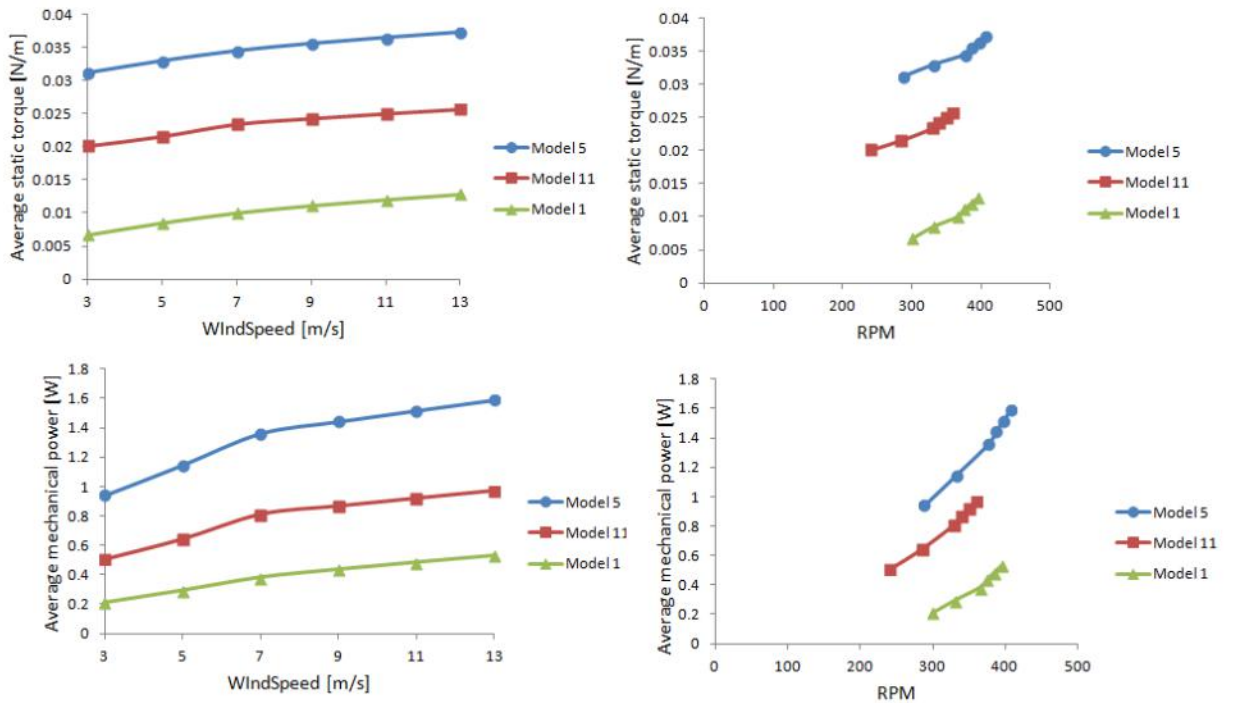


Figure 4.61: Comparison static torque and mechanical power of model 1, 5 and 11

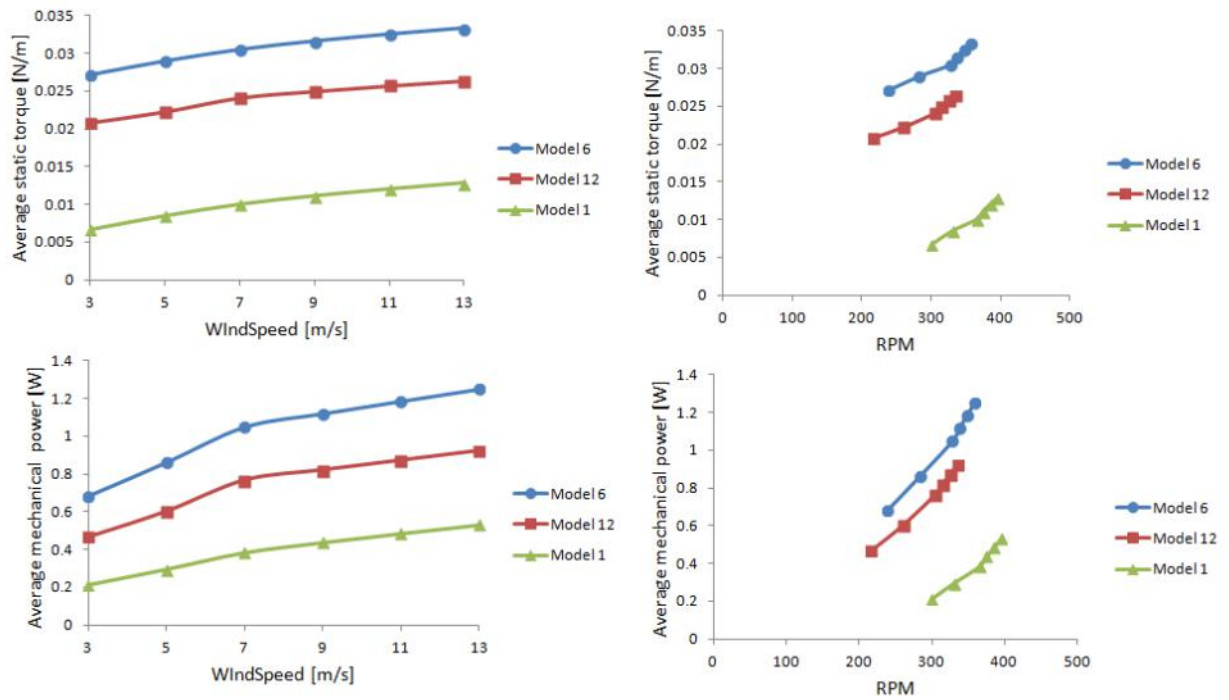


Figure 4.62: Comparison static torque and mechanical power of model 1, 6 and 12

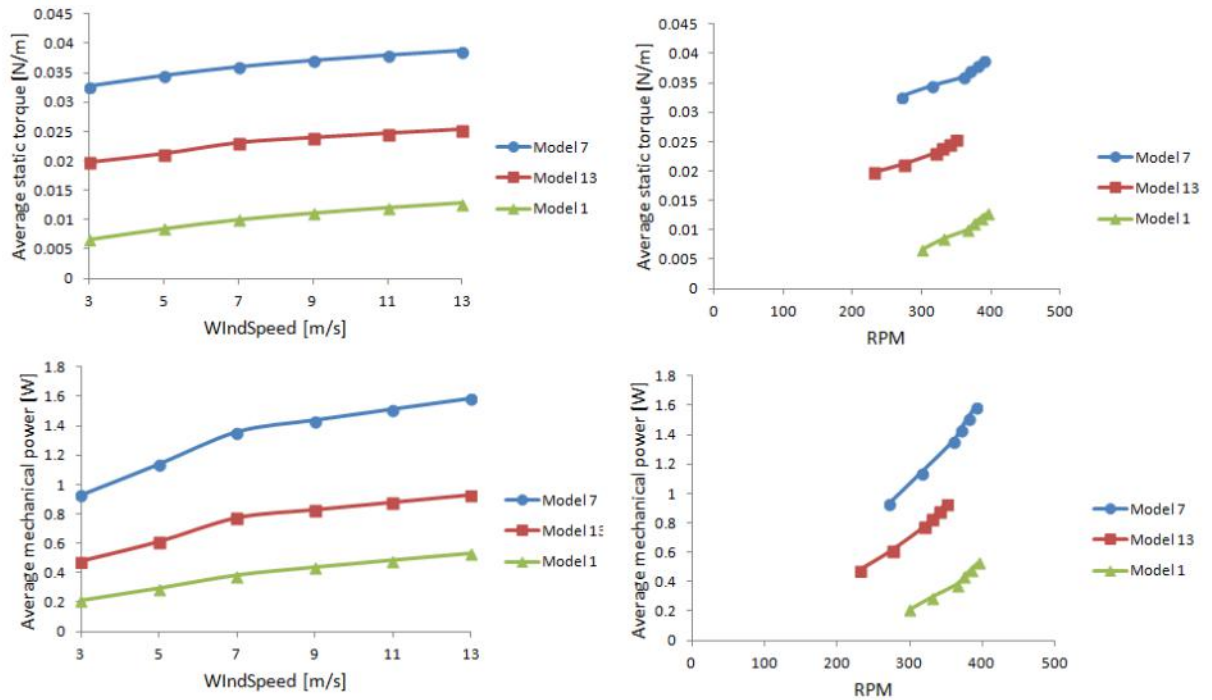


Figure 4.63: Comparison static torque and mechanical power of model 1, 7 and 13

CHAPTER 5

CONCLUSIONS AND FUTURE WORKS

Based on the investigate work, the objectives of the study project have been achieved. The important findings are summarized below.

5.1 Conclusions

The improvement of the performance of new design of the Savonius vertical axis wind turbine in low wind speeds ranges of 3 m/s to 13 m/s are studied experimentally. The effect of halves blade geometries and positions of these blades on the Mechanical power of new designs of the rotors are discussed in details. The experimental results obtained from this research are outlined below:

- It found that height of halves blades is the main factor that has a large influence on mechanical power of the new configuration of Savonius rotor with multiple halves blades.
- The closer the stacks blade (first new configuration of Savonius rotor) to the main blade, the more torque and power output.
- The results showed that Model 7 has higher static torque and mechanical power than other models of first configuration of rotors.
- For larger stacks blade, the fluid easily flows around the blades and as a result the torque output decreases
- Increasing in the height of halves blades leads to increase the weight of the rotor which decreases the static torque and mechanical power of rotors.
- The results obtained from these experiments showed that, the static torque at all the rotor angles for all unconventional Savonius rotors tested in this study are positive.
- It was also found that the largest halves bladed height, turbine shook violently during testing. At high wind speed and large blade rotors, the turbine is shook violently and unstable which leads to reduce the performance of the rotor.

5.2 Future Works

In order to make some improvement in the performances of unconventional Savonius rotors, there are some recommended actions that could be done to further improve the results calculated from this study:

- The materials of new design of Savonius wind turbine halves blade should be improved by using some lighter materials and more durable so that it could be able to withstand any high pressures caused by the wind for some period of time.
- Further research will aim at developing and optimizing the new design Savonius wind turbine under dynamic conditions. Also, the parameters of Savonius wind turbine rotor will be fully analyzed to enhance its effectiveness.

REFERENCES

- Altan, B., & Atilgan, M. (2012). A study on increasing the performance of Savonius wind rotors. *Journal of Mechanical Science and Technology*, 26(5), 1493-1499.
- Busby, R. L. (2012). *Wind power: The industry grows up*. Tulsa, OK: PennWell Corporation.
- Castellano, R. N. (2012). *Alternative energy technologies: Opportunities and markets*. Paris: Éd. des archives contemporaines.
- Chattot, J. J., & Hafez, M. M. (2015). *Theoretical and applied aerodynamics: And related numerical methods*.
- Chiras, D. D., Sagrillo, M., & Woofenden, I. (2010). *Wind power basics*. Gabriola Island, BC: New Society Publishers.
- Da, R. A. (2005). *Fundamentals of renewable energy processes*. Amsterdam: Elsevier Academic Press.
- Driss, Z., Mlayeh, O., Driss, D., Maaloul, M., & Abid, M. S. (2014). Numerical simulation and experimental validation of the turbulent flow around a small incurved Savonius wind rotor. *Energy*, 74, 506-517.
- Hardisty, J. (2009). *The analysis of tidal stream power*. Chichester, UK: Wiley.
- Hau, E., & Hau, E. (2006). *Wind turbines: Fundamentals, technologies, application, economics*. (Springer e-books.) Berlin: Springer.
- Jha, A. R. (2011). *Wind turbine technology*. Boca Raton, FL: CRC Press.
- Kamoji, M., Kedare, S., & Prabhu, S. (2009). Performance tests on helical Savonius rotors. *Renewable Energy*, 34(3), 521-529.
- Kishore, R. (2013). *Small-scale Wind Energy Portable Turbine (SWEPT)* (Master's thesis, State University).
- Lange, N., Grant, W., & Izaak Walton League of America. (1995). *Landowner's guide to wind energy in the Upper Midwest*. Minneapolis: Midwest Office, Izaak Walton League of America.
- Le, G. D. (2014). *Wind Power Plants: Theory and Design*. Pergamon.
- Ledec, G., Rapp, K. W., & Aiello, R. (2011). *Greening the wind: Environmental and social considerations for wind power development*. Washington, DC: World Bank.
- Lissaman, B., & Willson, R. (1974). *Applied Aerodynamics of Wind Power Machine*. Oregon State university.

- Magedi, M., Saad, M., & Asmuin, N. (2014). Comparison of Horizontal Axis Wind Turbines and Vertical Axis Wind Turbines. *IOSR Journal of Engineering*, 4(8), 27-30.
- Mahmoud, N., El-Haroun, A., Wahba, E., & Nasef, M. (2012). An experimental study on improvement of Savonius rotor performance. *Alexandria Engineering Journal*, 51(1), 19-25.
- Manwell, J. F., McGowan, J. G., & Rogers, A. L. (2011). *Wind energy explained: Theory, design and application*. Chichester: Wiley.
- Paraschivoiu, I. (2002). *Wind turbine design: With emphasis on Darrieus concept*. Montréal: Polytechnic International Press.
- Prentis, J. (1977). *Energybook 2: More natural sources & backyard applications*. Philadelphia: Running Press.
- Rogowski, K., & Maroński, R. (2015). CFD computation of the Savonius rotor. *Journal of Theoretical and Applied Mechanics*, 37.
- Sayigh, A. (2015). *Renewable Energy in the Service of Mankind Vol I: Selected Topics from the World Renewable Energy Congress WREC 2014*. Cham: Springer International Publishing.
- Sharma, A., & Kar, S. K. (2015). *Energy sustainability through green energy*. India: Springer.
- Sharma, S., & Sharma, R. K. (2016). Performance improvement of Savonius rotor using multiple quarter blades – A CFD investigation. *Energy Conversion and Management*, 127, 43-54. doi:10.1016/j.enconman.2016.08.087
- Soliman, M. (2011). *Designing, Manufacturing And Testing For Modified Vertical Axis Wind Turbine (Giomill)* (Master's thesis). Retrieved from ProQuest Dissertations and Theses database.
- Steeby, D. (2012). *Alternative energy: Sources and systems*. Clifton Park, NY: Delmar, Cengage Learning.
- Steven, P. (2004). "Another Approach to Wind. Retrieved from <http://www.windturbine-performance.com/www/another%20approach%20to%20wind-apptowind.html>
- Sun, X., Chen, Y., Cao, Y., Wu, G., Zheng, Z., & Huang, D. (2016). Research on the aerodynamic characteristics of a lift drag hybrid vertical axis wind turbine. *Advances in Mechanical Engineering*, 8(1), 168781401662934.

- Tong, W. (2010). *Wind power generation and wind turbine design*. Southampton: WIT Press.
- Turner, W. C. (2005). *Energy management handbook: By Wayne C. Turner*. Lilburn, GA: Fairmont Press.
- Wizelius, T. (2006). *Developing Wind Power Projects: Theory and Practice*. Florence: Taylor and Francis.